MICROCOPY RESOLUTION TEST CHART
NATIONAL BUREAU OF STANDARDS 1963 A

UNLIMITED

AD A044987

ROYAL AIRCRAFT ESTABLISHMENT

∗

Technical Report 77025

A FAST RESPONSE THRUST TRANSDUCER FOR GASDYNAMIC THRUSTERS

by

B.C. Barber

∗
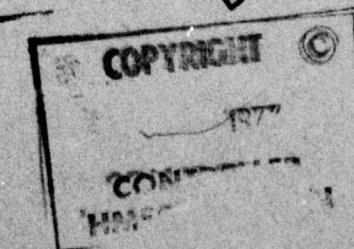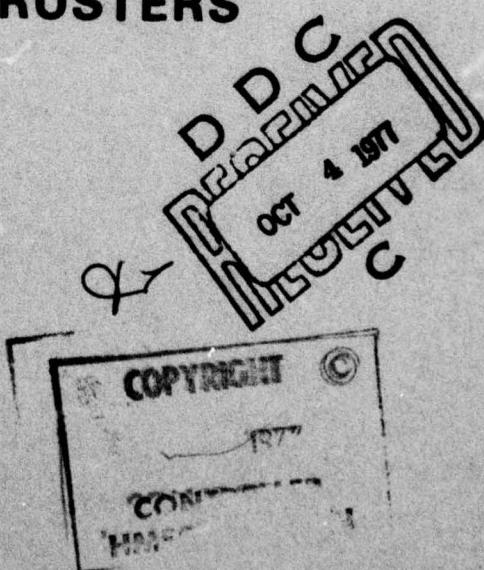
**Procurement Executive, Ministry of Defence**
Farnborough, Hants

UNLIMITED

AD No.
DDC FILE COPY

REPORT DOCUMENTATION PAGE

Overall security classification of this page

UNCLASSIFIED

As far as possible this page should contain only unclassified information. If it is necessary to enter classified information, the box above must be marked to indicate the classification, e.g. Restricted, Confidential or Secret.

1. DRIC Reference (to be added by DRIC)	2. Originator's Reference RAE TR 77025 ✓	3. Agency Reference N/A	4. Report Security Classification/Marking UNCLASSIFIED

5. DRIC Code for Originator 850100	6. Originator (Corporate Author) Name and Location Royal Aircraft Establishment, Farnborough, Hants, UK

5a. Sponsoring Agency's Code N/A	6a. Sponsoring Agency (Contract Authority) Name and Location N/A

7. Title A fast response thrust transducer for gasdynamic thrusters

7a. (For Translations) Title in Foreign Language

7b. (For Conference Papers) Title, Place and Date of Conference

8. Author 1. Surname, Initials Barber, B.C.	9a. Author 2	9b. Authors 3, 4	10. Date February 1977	Pages 49	Refs. 9

11. Contract Number N/A	12. Period N/A	13. Project	14. Other Reference Nos. Space 517

15. Distribution statement
  (a) Controlled by – MOD(PE) DRASA ASA 4

  (b) Special limitations (if any) –

16. Descriptors (Keywords)   (Descriptors marked * are selected from TEST)

Thruster instrumentation. Propulsion. Attitude control

17. Abstract

    Problems associated with the measurement of the thrust and impulse of short pulses (20-100 ms) of low thrust (about 100 mN) electrothermal hydrazine thrusters are discussed. Thrust pulses measured by a conventional transducer are distorted by the self-excitation of mechanical and acoustic resonances present in the thruster and thrust transducer.

    A technique for mitigating the effects of these resonances is described. This technique involves transforming the electrical signal from the thrust transducer in real time by an analogue network which has a transfer function which is the inverse of the transfer function of the thruster-thrust transducer system.

    Results are presented showing the transient thrust measurement of an electrothermal hydrazine thruster.

RAE Form A143

UDC 629.19.014.6 : 621.455.2 : 547.298.62 : 621.317.39

(14) RAE-TR-77025

ROYAL AIRCRAFT ESTABLISHMENT

(9) Technical Report 77025

Received for printing 17 February 1977

(6)

A FAST RESPONSE THRUST TRANSDUCER FOR GASDYNAMIC THRUSTERS.

by

(10) B. C. Barber   (11) 7 Feb 77

(12) 51 p.

SUMMARY

Problems associated with the measurement of the thrust and impulse of short pulses (20-100 ms) of low thrust (about 100 mN) electrothermal hydrazine thrusters are discussed. Thrust pulses measured by a conventional transducer are distorted by the self-excitation of mechanical and acoustic resonances present in the thruster and thrust transducer.

A technique for mitigating the effects of these resonances is described. This technique involves transforming the electrical signal from the thrust transducer in real time by an analogue network which has a transfer function which is the inverse of the transfer function of the thruster-thrust transducer system.

Results are presented showing the transient thrust measurement of an electrothermal hydrazine thruster.

Departmental Reference: Space 517

310 459

2

LIST OF CONTENTS

1   INTRODUCTION

Recently proposed attitude control systems employ electrothermal thrusters in a wheel dumping mode[1]. These thrusters operate for times of the order of hundreds of milliseconds at thrust levels of 100-200 mN. They are also usually designed to operate at greatly reduced impulse bits with pulse widths of tens of milliseconds to maintain attitude control in the event of the wheel system failing, thus providing a backup system. The fastest electrothermal thrusters appear to have plenum pressure rise times of the order of 10 ms and fall times of 20 ms (Ref 2). Thrust rise/fall times would be expected to be of the same order. At low plenum pressures the nozzles of small thrusters are usually inefficient due to excessive boundary layer growth; this manifests itself as a loss in specific impulse at low pressures. Therefore for pulse widths of tens of milliseconds, the thruster is operating at a low specific impulse over a significant proportion of the pulse. The thrust rise and fall times are therefore important parameters and a thrust measuring system for use with these short thrust pulses must have an adequate bandwidth.

Thrust information may be obtained from plenum pressure measurements. However because of the inefficiency of the nozzle during the pressure rise and fall one must take into account the variation of the nozzle discharge coefficient with pressure. In the steady state condition the boundary layer is usually small (nozzle discharge coefficient of ~0.95 or so), but in the transient condition the nozzle efficiency can be very low during the pressure rise (and fall). This, of course, depends to a large extent on the nozzle parameters, operating pressure, temperature etc. Thus when the pressure rise and fall occupy a significant fraction of the total pulse length, thrust (and impulse) information from plenum pressure measurements is likely to be misleading.

In addition assumptions must be made regarding the composition and thermodynamic properties of the exhaust. Furthermore the necessity of making provision for a pressure tapping on the plenum can be a great nuisance, and the location of the tapping and the gasdynamics at the tapping can have a great bearing on the veracity of the pressure measurement. It is therefore desirable to develop a technique for measuring thrust directly.

The most reliable approach is to measure the thrust with a fast response thrust transducer and this is the approach adopted here. This solution has other attractions. By integrating the thrust over the pulse width the impulse may be evaluated directly, and the impulse produced by a train of pulses may be

evaluated, as may the impulse produced by any individual pulse in a pulse train. Other impulse measuring techniques, eg a ballistic pendulum, do not have this flexibility. Furthermore, certain types of thruster (principally those operating with hydrazine propellant) can develop 'roughness' and it is desirable to be able to measure these thrust perturbations.

A system rise-time of 2.5 ms corresponds to a bandwidth (to -3 dB) of about 150 Hz for a Gaussian filter and would result in an error of about 3% in the measurement of a 10ms rise time, assuming that the rise times add as the root of the sum of their squares. The plenum pressure oscillations present in these thrusters appear to cover a frequency band from 50 Hz to 150 Hz, and the thrust oscillations will cover a similar band. The optimum system rise time is therefore about 2.5 ms.

2   THRUST AND IMPULSE MEASURING TECHNIQUES

Thrust measuring transducers must essentially be mass-spring systems with the thruster forming part of the mass. The 'spring' force may be a restoring force provided by gravity, by a mechanical spring, or by an electromechanical actuator in the case of a force-feedback system. To achieve a given bandwidth for time-resolved measurements, the system must either have a fundamental resonant frequency for above the required frequency band with associated damping and/or filtering, or a fundamental within the frequency band with the displacement signal processed by a transformation technique. Systems which have a high resonant frequency can work well when the thruster has a relatively high thrust and low mass. Recent thrusters, however, often have masses of several hundred grams. In such cases to achieve the required resonant frequency (several hundred Hertz for a 2.5 ms rise time) the transducer has to be so stiff that the displacement is less than 10^{-8} m at the operating thrust levels. It is very difficult to measure such a small displacement reliably because of temperature fluctuations and creep. Such a transducer using a piezoelectric element to measure displacement and provide the (spring) restoring force has been constructed. It has been found to have dc stability problems. The frame of the transducer distorts and creeps very slightly and causes considerable drift. The most sensitive charge amplifier/piezoelectric transducer combination available has to be operated beyond its capabilities with the result that charge amplifier drift can easily exceed the measured thrust. In addition there is the usual charge leakage associated with all piezoelectric transducers. Force-feedback systems have other problems. Experience has shown that mechanical resonances present in the thruster are excited by the actuator providing the feedback force.

In fact these mechanical resonances appear as LCR networks within the feedback loop and cause severe stability problems. The resonances may be integrated by including networks with suitable transfer fractions within the feedback loop, but these networks invariably become very complex and difficult to formulate. Moreover, each thruster must be treated individually.

Inverse transfer function techniques allow the transducer to have a low resonance (within the frequency band of interest) and in consequence, a much greater sensitivity. The stiffness of a mass spring system is proportional to the square of the natural frequency, so that reducing the fundamental from, say, 200 Hz to 20 Hz increases the sensitivity by a factor of 100. Because displacements are of a reasonable magnitude (of the order of a micron in the case of the present thrust transducer), temperature fluctuations and creep difficulties become insignificant. In fact with the present transducer there have been no problems with dc stability. Moreover, such a technique is of an open loop character and there are no feedback stability problems.

3   THE INVERSE TRANSFER FUNCTION TECHNIQUE

If the torque presented to the transducer is $T(t)$, the spring torque constant is k , the damping factor is c , and the moment of inertia I , the equation of motion for a torsional mass-spring system (ie the thrust transducer) is

$$I\ddot{\theta} + c\dot{\theta} + k\theta = T(t) \ . \qquad (1)$$

The angular displacement θ may be measured by a displacement transducer. This signal is operated on using operational amplifier techniques to give the three terms $I\ddot{\theta}, c\dot{\theta}$ and $k\theta$. These terms are then summed to give $T(t)$, which, apart from a numerical constant, is the required thrust function. $T(t)$ is finally filtered to remove noise and define the system bandwidth. From the standpoint of the operational calculus one is, of course, setting up the inverse of the transfer function of the mechanical system. Hence the term 'inverse transfer function'. If the mechanical system has little damping it is possible to ignore the velocity term $(c\dot{\theta})$. The acceleration term $I\ddot{\theta}$ may then be derived from an accelerometer attached to the thruster. This technique is known as 'accelerometer compensation' and has been employed on rocket motor thrust stands measuring thrusts of the order of 250 N (Ref 3) and 5000 N (Refs 4-6).

The thruster force, as derived from the inverse transform, is usually distorted by small oscillations derived from the mechanical resonances present

6

in the thruster. This is a result of approximating an essentially multi-degree of
freedom system by a single degree of freedom. It is possible to remove these
distortions by introducing further inverse transfer functions and this technique
will be described in a later section. Alternatively, these distortions may be
removed by filtering. To avoid introducing any overshoot or ringing into the
electronic circuitry, the filter must be of a type having a linear phase charac-
teristic. Such filters unfortunately have a very slow amplitude cut-off[7] and
unnecessarily limit the bandwidth. The cut-off may be made more rapid without
unduly distorting the phase response by introducing zeros into the stopband[8].
This has the advantage that if a particular resonance is troublesome it may be
removed by introducing a zero at that frequency. This is only possible, of
course, if the resonance lies above the passband. It has been found that this is
often the case and so recourse to further inverse transforms has often proved
unnecessary.

4   THE THRUST TRANSDUCER MECHANICAL DESIGN

The mechanical part of the transducer is shown in schematic form in Fig 1
and installed in a vacuum chamber in Fig 2. The thruster is rigidly mounted on
an aluminium alloy platform measuring 160 mm long, 180 mm wide, and 6 mm deep.
The platform is mounted onto the mainframe of the transducer by two torque tubes.
Each torque tube has a length of 35 mm and an inside diameter 2.5 m with a wall
thickness of 0.25 mm over a length of 5 mm. The torque tube is shown in Fig 3.
They are made from 14% tungsten vanadium tool steel and fully heat treated, and
appear to be compatible with hydrazine, at least for intermittent use. One tube
carries the propellant and the other the electrical wires. This arrangement
ensures that the propellant flows along the axis of rotation. There can thus be
no spurious effects caused by the propellant pressure and viscosity and both
liquid and gaseous propellants can be accommodated. Moreover this arrangement
has a very high lateral rigidity and helps to ensure that the transducer has only
a single degree of freedom. In this connection it is essential to ensure that
the clamps holding the torque tubes to the platform and to the mainframe are very
rigid and that the tubes are mounted on the same axis to avoid bending.

The thruster provides a torque which rotates the platform against the
restoring force of the torque tubes. This rotation is measured by a capacitive
transducer mounted on the mainframe and acting on an arm rigidly attached to the
mainframe. The space between the coil and magnet is filled with silicon vacuum
oil which provides a small amount of damping. Silicon oil is an ideal choice
since it retains an almost constant viscosity up to quite high temperatures –

the platform can become quite hot if there is a large heat flux leakage from the hot thruster to its mounting.

The coil operates in the same way as a loudspeaker coil and is used to calibrate the transducer dynamically. Current pulses of known shape are fed through the coil and the inverse transform adjusted until the indicated force is the same as the input.

Very great care is needed in the design of the transducer to avoid mechanical resonances within the frequency band of interest. All fittings and fixtures have to be made very rigid. The platform in particular can have many resonances and the present dimensions were arrived at after considerable calculation and experimentation. In the present design the most serious resonance is a lateral oscillation of the whole platform up and down caused by the torque tubes bending and stretching very slightly. Fortunately this resonance occurs at from 600 Hz to 750 Hz depending on the mass of the thruster, and is well outside the 0 to 200Hz band. The thrust transducer is very sensitive to ground vibrations and in order to reduce these as far as possible the transducer mainframe is hung on eight coil springs. The transducer weighs some 40 kg and this mass in conjunction with the springs forms an *effective low-pass* mechanical filter. The movement of the frame under the influence of a 100mN thruster is completely undetectable. The frame itself measures about 400 mm long, 230 mm wide and 70 mm deep. It is constructed from mild steel plate 9 mm thick and is nickel plated. The purpose behind such a heavy construction is to make the mainframe very rigid to eliminate resonances and to avoid any creep or distortion. In addition the displacement transducer requires very heavy screening. Parts of the displacement circuit operate at high impedance - of the order of 10^8 Ω and it is essential that there is no pick up from stray 50 Hz fields. Due to skin effect the mainframe has a thickness of about four skin depths at a frequency of 50 Hz, and 50 Hz fields are attenuated in amplitude by a factor of about 0.02 inside the mainframe.

5   THE THRUST TRANSDUCER ELECTRONICS

The thrust transducer electronics are divided into three units, the mainframe unit, the control unit and the inverse transfer function unit. The mainframe unit is contained within the chassis of the thrust transducer and comprises the displacement transducer, battery and control relays. This unit is connected to the control unit via two cables, one carrying the displacement signal and the other the control signals. Block diagrams of the three units are shown in Figs 4, 5 and 6 and are self explanatory. The various circuits contained in the three units are briefly reviewed in the remainder of this section.

5.1   The displacement transducer

It is essential that the electrical noise present in the displacement circuitry be kept as low as possible. This is because the signal is operated on by the inverse transfer function containing a double differentiator which is very sensitive to noise. Commercial displacement transducers were found to be too noisy so a transducer was specially developed. The overall schematic is shown in the block circuit Fig 4, and the transducer probe is shown in Fig 7. The capacitive transducer is connected in a feedback loop around the amplifier. A guard ring around the centre electrode of the probe ensures linearity.

The gain of this feedback configuration = $(-c_1/c_2)$; c_1 is constant (at about 0.5 μμF) and c_2 is the feedback capacitance, in this case the capacitance between the probe and arm bolted to the platform. The capacitance of the probe and arm = k/d where k is an arbitrary constant and d is the probe-arm separation. Hence if a constant ac signal is applied to c_1 the output voltage is directly proportional to d .

The voltage regulator and oscillator circuit is shown in Fig 8. The regulator ensures a constant output irrespective of supply voltage. The fet is biased at a point at which its change in mutual conductance with temperature is a minimum and this ensures a constant output irrespective of temperature. Temperature-voltage output curves for two samples of regulator and oscillator are shown in Fig 9 and temperature-frequency curves for the same samples in Fig 10. The oscillator holds its output to within 0.5% up to 110°C.

The high gain amplifier schematic is shown in Fig 11. The amplifier has a gain of about 70 dB at 10 kHz (the oscillator frequency). The gain is tailored to fall off either side of 10 kHz at 6 dB/octave. The high frequency cut-off is achieved by c_2 and the low frequency cut-off by c_1 . The gain becomes unity at about 20 MHz where the cut-off slope becomes 10 dB/octave and at the low frequency end the gain becomes unity at about 3 Hz. This ensures loop stability. The amplifier is somewhat novel in that the gain is achieved in only one stage (Tr 2) by using a constant current fet (fet 3) as the collector load of Tr 2.

The oscillator and amplifier are contained within the mainframe of the unit and are powered by an integral 25V rechargeable battery which can be recharged at will (via SW 2 see Fig 5) from the control unit. During normal operation the battery amplifier and oscillator are isolated from external circuitry including the output which is transformer coupled to the demodulator. These precautions were found necessary to eliminate 50 Hz noise pick-up from the power lines and

earth loops. The displacement transducer has a measured linearity of 0.2% up to full scale deflection. The oscillator holds its output within 0.5% to 110°C and then a static load can be measured to within 1% under any conceivable circumstance.

5.2   The rectifier

The output from the displacement transducer is in the form of an amplitude modulated 10.5 kHz carrier. This is rectified by the circuit shown in Fig 12. This is a conventional operational amplifier full-wave rectifier circuit. Input and output waveforms for the rectifier are shown in Fig 13 for a 1V peake-to-peak 10kHz sine wave modulated 50% by a 1kHz sine wave.

5.3   The demodulator filter

The demodulator filter circuit is shown in Fig 14. The frequency response of the filter is shown in Fig 15. At a frequency of 20 kHz (the principal component of the rectified signal) the attenuation is over 100 dB. The filter is an eighth order linear phase filter and is the passive realisation of the active filters described in Ref 8. The filter has a rise time of 0.28 ms with an over-shoot of 1%.

5.4   The meter circuit

The meter has three functions, it is used in setting up and calibrating the transducer, in measuring steady thrust, and in indicating the battery voltage. The meter circuit consists of the digital panel meter, its buffer amplifiers and the clock. The clock operates the meter at 500ms intervals and is synchronised with the pulse calibrator as explained in the next section. The circuit is entirely conventional.

5.5   The calibrator

The calibrator schematic is shown in Fig 16. It consists of a standard voltage to current converter circuit from the clock. A 2Hz square wave is applied to the drive amplifier which drives a corresponding current through the coil attached to the transducer platform (see Fig 1). The coil movement is typically of the order of 1 μm and can thus be considered to move in a region of constant magnetic flux. Hence the force applied by the coil to the platform is directly proportional to the current. This enables the transducer to be set up and calibrated as explained in section 6.

5.6   The output filters

The output filters are two filters referred to as 'filter A' and 'filter B' in Fig 6. They have three functions; they define the system bandwidth, they remove high frequency noise and they remove high frequency oscillations derived from small mechanical resonances in the thruster and thrust transducer. These oscillations are a result of approximating an essentially multi-degree of freedom system by a single degree of freedom. It is possible to remove these distortions by introducing further inverse transforms (see Appendix) and/or by filtering. To avoid introducing any overshoot or ringing into the electronic circuitry the filter must be of a type having a linear phase characteristic. Unfortunately such filters have a very slow amplitude cut-off and unnecessarily limit the bandwidth. The cut-off may be made more rapid without unduly distorting the phase response by introducing zeros into the stop band. This has the advantage that if a particular resonance is troublesome it may be removed by introducing a zero at that frequency. This is only possible, of course, if the resonance lies above the pass band. When this is the case recourse to further inverse transforms is unnecessary.

The circuit of both filter A and filter B is shown in Fig 17. In a typical case filter A was designed to have a cut-off frequency of 230 Hz and filter B a cut-off frequency of 130 Hz. The overall frequency response of the two filters connected in series is shown in Fig 18. There are zeros at 300 Hz, 570 Hz, 655 Hz and 1.15 kHz. The rise time of the two filters was 2.5 ms with overshoot <1% (unmeasurable).

5.7   The inverse transfer function

The schematic of the inverse transfer function is shown in Fig 19. Differentiators, and particularly double differentiators can be unstable since their gain increases with frequency. It is therefore necessary to modify the response of a practical differentiator by curtailing its gain at high frequency. This is done in this circuit by including the resistors r in series with the capacitors c_1 and c_2 . The corner frequency of the differentiators is set at about 1 kHz - well outside the band edge of the filters. Hence the circuit accurately reproduces the required transfer function within the pass band. The damping and inertia coefficients are set separately by R_3 and R_5 . By arranging the gains of each differentiator to be set in this way it is possible to calibrate R_3 and R_5 . The undamped natural frequency of the transducer is measured and set up on the R_3 dial and the R_5 dial set to kn^2 where k is a calibration constant and n the natural frequency. The damping oil is added and the inverse transfer function and transducer are ready for operation.

5.8   The battery control circuit

The battery in the transducer mainframe is switched by relays RL1 and RL2 (Fig 4). The battery is divided into two halves. When SW 2 is in the on position the two halves are connected in series and connected to the displacement transducer. When SW 2 is in positions 1, 3 and 4 the two halves are connected in parallel and connected to the control unit. In position 4 the battery is, in addition, connected to the -15V and +15V lines through a current regulator shown in Fig 20. The current is set at 90 mA and the battery takes about 15 hours to charge fully.

6   CALIBRATION AND SETTING THE INVERSE TRANSFER FUNCTION

Calibration is performed by applying a known torque to the platform. This is achieved by passing a 2Hz square current waveform through a coil mounted on the platform as explained in section 5.6. The exact current is for the required torque (± 10 mN m) is obtained by hanging weights from the platform and determining the deflection. When the current has been determined the calibrator amplifier gain is determined and the 'calibrator' has been 'calibrated'. The deflection of the platform under the influence of a rectangular force waveform is shown in Fig 21. The steady state deflection corresponding to the calibrated force is measured by the meter. This is obtained by waiting until the platform oscillations have been damped to an acceptable level and then triggering the meter. The meter samples the waveform at a quasi steady level and holds the reading until the same point on the next cycle. The meter scaling circuit is adjusted until the meter needs a convenient value corresponding to the calibrated torque (10 mN m). The waveforms corresponding to the process are shown in Fig 21. The top trace is the driving current (ie the force), the middle waveform the corresponding displacement and the bottom waveform, the meter sample signal.

This calibration technique ensures that the transducer calibration may be checked before or at any time during a series of tests merely by throwing one switch. Moreover a calibrated waveform is available for external recording apparatus.

The inverse transfer function is also set up by using the calibration waveform. The displacement signal corresponding to the calibrator current waveform is the input to the inverse transfer function (ITF). If the ITF is set up properly then it will remove the effects of the thrust transducer, ie the ringing and slow response, and the output will correspond with the original calibrator current waveform. An oscilloscope is used to observe the calibrator waveform

and the output of the ITF. The output of the velocity channel of the ITF is initially made as low as possible by increasing R_3 (see Fig 19) to its maximum value. The output of the acceleration channel is then adjusted (R_5) until the output of the ITF corresponds approximately with the calibrator waveform. The velocity channel is then adjusted and so on until the output corresponds as closely as possible with the calibrator waveform. This method of adjustment is stable and convergent. Fig 22 shows the various waveforms when the ITF is set up. The velocity signal corresponds to point A in Fig 19 and the acceleration signal to point B. It can be shown that when the ITF is set up with one input then it is automatically valid for all input waveforms (within its bandwidth).

7   OPERATION OF THE TRANSDUCER WITH A THRUSTER

Most thrusters have a propellant flow control valve attached. This valve can produce considerable reaction forces. The pulses in Fig 23 are reaction transients produced by a small flow control valve. The first two spikes correspond to the valve opening and the last two to the valve closing. The interval between the valve opening and closing is nominally 100 ms and the peak amplitude of the spikes is 70 mN. The first downward spike is caused by the valve armature accelerating away from the valve seat and producing a reaction force on the force transducer. This reaction reverses when the armature slows down at the end of its travel and this is the next upward spike. The situation is reversed when the valve closes except that the last downward spike has a double peak showing that the valve armature bounces off the valve seat.

These reaction forces distort the leading and trailing edges of the thrust pulses. Furthermore the reaction spikes tend to excite resonances on the thruster and these distort the thrust pulse even more. Fig 24 shows the thrust produced by a small thruster having a rise time of about 12 ms and producing a thrust of about 60 mN with a nominal pulse width of 30 ms. The system rise time in this case is 2.5 ms. Fig 25 shows the same thrust pulse but with a system rise time of 5 ms obtained by switching further filters. The valve reaction spikes are clearly visible as is the effect of reducing the bandwidth. Fig 25 shows a much cleaner trace than Fig 24, but at the expense of slightly slowing up the observed rise and fall. The amplitude of the valve reaction spikes in Fig 25 is also much reduced. Apart from the spikes the trace shows the typical exponential rise-exponential fall pulse obtained from gasdynamic thrusters.

Fig 26 shows the thrust obtained from a small resistojet. This particular thruster has a large number of resonances and these distort the trace considerably. The thrust amplitude is 50 mN and the pulse width is 45 ms. The time

constant of the exponential rise and fall is about 10 ms. The resonances are
excited by the valve spikes which are visible but buried in the noise. It is
possible to separate the valve from the thruster and mount the valve onto the
mainframe of the transducer. This, however, increases the time constant of the
thrust pulse since extra pipe volume is introduced between the thruster and valve.
Fig 27 shows the various components of the inverse transform signal corresponding
to the thrust pulse in Fig 25. The top trace is the displacement of the platform.
In this case the platform was completely undamped. The middle trace is the output
of the acceleration channel and the bottom trace, traces 1 and 2 summed and
filtered. In this case there was no damping and hence the velocity channel was
not used. It is quite possible to use the system completely undamped, but
repetition pulsing can cause problems if the natural frequency of the transducer
approaches a harmonic of the thruster repetition frequency. It is usually best
to provide for a small amount of damping and Fig 28 shows the outputs from the
various channels in such a case. The pulse has a width of 100 ms and an ampli-
tude of 100 mN. The thruster shows rise and fall times of about 15 ms. The top
trace is the displacement of the platform, the second trace the output of the
velocity channel, the third trace the output of the acceleration channel and the
bottom trace is the thrust pulse and is the sum of the top three traces. Note
that the phase difference between the oscillations in the first and third traces
is 180° and the phase difference between the displacement and velocity channels
is 90°. It will be noted in Fig 28 that the thrust does not settle back down to
zero until about 250 ms after the end of the pulse. It is thought that this
'tail' is caused by gas within the thruster slowly leaking out of the nozzle
after the main bulk of the propellant has been exhausted.

Fig 29 shows the thrust produced by a small electrothermal hydrazine
thruster. The top trace shows the thrust and the bottom trace shows plenum
pressure. This particular thruster had a comparatively long response time and
the pulse length is 2 s. The mean amplitude of the thrust is about 120 mN and
the mean pressure about 517 kN m^{-2} (75 psia). There is a very strong correlation
between the thrust transients and pressure transients, not only for the slow
transients but also at high frequencies (>50 Hz). Unfortunately the printing
process removes the fine detail from photographs so Fig 29 does not show the high
frequencies too well and the valve reaction spikes, visible on the original, are
not reproduced. In order to obtain the result shown in Fig 29 it was necessary
to use inverse transfer functions of a higher order than the simple ITF described
in section 3. The techniques employed in this case are explained and described
in the Appendix.

8   IMPULSE MEASUREMENT

The impulse corresponding to a particular thrust pulse is obtained simply
by integrating the thrust pulse. Fig 30 shows a type of track and hold integrator
which has been used to obtain the impulse data shown in Figs 23, 31 and 32.
Fig 30 is a standard integrator except for the inclusion of c_1 . Under quiescent
conditions relay contacts 1a and 1b are closed. Thus the integrating capacitor
c and capacitor c_1 charge to the standing dc potential at the integrator input
(the output of the integrator remaining at zero). When the circuit is required
to integrate contacts 1a and 1b open. The integrator then only integrates any
change in input voltage. This eliminates any need to set the standing dc
potential at the integrator input to zero. The amplifier must, of course, have
a very low input current requirement (an fet input operational amplifier), other-
wise c_1 would change its charge during the integration.

The lower trace of Fig 23 shows the impulse produced by the valve reaction
spikes. The maximum impulse at any point is about 2.5 µN s and over one complete
operation the impulse sums to zero, as it should. Fig 31 shows the impulse
produced by a succession of 100 ms pulses of about 110 mN amplitude. The total
impulse produced by the pulses is about 59 mN s. Fig 32 shows the impulse pro-
duced by just one of the same pulses. The indicated impulse is 10 mN s.

9   CONCLUSION

It has been demonstrated that techniques used for the dynamic thrust
measurement of rocket motors can be applied successfully to small thrust stands
measuring thrusts some five orders of magnitude smaller with adequate system
rise times. Problems exist with mechanical resonances, present in these thrusters,
being excited by reaction spikes from the propellant control valve. However these
second order distortions can be removed by further inverse transforms (see the
Appendix). Impulse data is readily obtained from the thrust transducer by
integrating the output. Furthermore the impulse measurements are unaffected by
the valve reaction transients since these are internal forces.

Appendix

INVERSE TRANSFER FUNCTIONS FOR MULTI-DEGREE OF FREEDOM SYSTEMS

When a system such as the thrust transducer has only one degree of freedom it is straightforward to explain the operation of the inverse transfer function in terms of a single differential equation (see section 3). When there are several degrees of freedom, however, such an explanation is not possible and recourse to systems theory is necessary. It is the purpose of this Appendix to explain how inverse transfer functions may be used to remove the effects not only of the fundamental oscillation of the transducer platform, but also of the multitudinous mechanical resonances present on the thruster and transducer. An explanation is given of how this technique was applied to a small hydrazine thruster to obtain the thrust data shown in Fig 29.

The thrust transducer and thruster can be regarded as a linear system with one input (the thrust function) and one output (the transducer displacement). This system is a dynamical system and a number of differential equations may be written which govern its operation. In the particular case of the thrust transducer without the thruster a satisfactory approximation may be made by assuming only one degree of freedom and one governing differential equation:

$$(Ip^2 + cp + k)\theta(t) = \tau(t) \tag{2}$$

or

$$\theta(t) = A(p)\tau(t) \tag{3}$$

where I is the moment of inertia of the transducer, k is a measure of the torque tube stiffness and c is a damping coefficient. $\theta(t)$ is the angular rotation of the platform, $\tau(t)$ the torque caused by the thruster $A(p)$ is a differential operator - the 'system operator', p corresponds to differentiation with respect to time.

The system $A(p)$ has an inverse $A^{-1}(p)$, and it can be shown[9] that provided both $A(p)$ and $A^{-1}(p)$ start in a 'zero state' then

$$A(p)A^{-1}(p) = A^{-1}(p)A(p) = I . \tag{4}$$

In the case of $A(p)$ and $A^{-1}(p)$ 'zero state' means 'zero energy', ie the thrust transducer has to have no initial energy and neither does its inverse. The

product $A^{-1}(p)A(p)$ corresponds to a tandem connection of the two systems the order of operation being from right to left that is $A(p)$ operates before $A^{-1}(p)$. Now

$$\theta(t) = A(p)\tau(t)$$

so

$$A^{-1}(p)\theta(t) = A^{-1}(p)A(p)\tau(t)$$

$$= \tau(t) .$$

So that operating on the output of the transducer $\theta(t)$ by the inverse system operator $A^{-1}(p)$ produces the impulse function $\tau(t)$. This is just an alternative explanation of the inverse transfer function to the one given in section 3. And in the case of the thrust transducer $A(p)$ has the form:

$$A(p) \equiv 1/(Ip^2 + cp + k) \tag{5}$$

and its inverse $A^{-1}(p)$ is

$$A^{-1}(p) \equiv Ip^2 + cp + k . \tag{6}$$

The practical realisation of A^{-1} is shown in Fig 19. In principle the effects of any system may be removed by operating on the output signal by a circuit having the inverse operation. There are limitations, however $A(p)$ must have a stable inverse. In the case of the linear dynamical systems described here, this is true. Further A^{-1} must not be anticipative, that is, it is not possible to construct the inverse of a pure time delay since this would involve time reversal – a regrettably impossible feat.

In general a system such as the thrust transducer-plus-thruster has more than one degree of freedom, and there will be a number of governing differential equations. In such a case, provided that initially the system is in a zero state, it can be shown that the corresponding system operator is of the form:

$$B(p) \equiv \sum_{i=0}^{n} \alpha_i p^i \bigg/ \sum_{j=0}^{m} \beta_j p^j \tag{7}$$

and, of course, the inverse is:

$$B^{-1}(p) \;\equiv\; \beta_j p^j \big/ \alpha_i p^i \tag{8}$$

where the summation signs have been omitted. The magnitude of n and m is dependent not only on the number of degrees of freedom but also on the precise nature of the system, as are the constants α_i, β_j .

The two main problems in the application of the inverse operator technique are the evaluation of the constants in (7), ie evaluating the system, and the practical realisation of the inverse system B^{-1} . There are at least three ways of setting up $B(p)$ for a system. One is through direct analysis and the other two involve determining the transfer function either from the impulse response or from sinusoidal response. Direct analysis is not practicable and the impulse response technique is not easy to analyse. Probably the only satisfactory technique when the system is of a complex nature is to plot the amplitude-frequency and phase-frequency characteristics of the system. In principle, given these characteristics the constants $\alpha_i \beta_j$ in equation (7) may be evaluated.

Taking the Laplace transform of (7) we have:

$$B(s) \;=\; \alpha_i s^i \big/ \beta_j s^j \tag{9}$$

$B(s)$ is known as the transfer function of the system $B(p)$ and the inverse transfer function is $B^{-1}(s)$. Now the frequency response of a system is determined by its transfer function $B(s)$ and it is straightforward to show that the frequency response of a combination of a transfer function $B(s)$ and its inverse $B^{-1}(s)$ is flat from zero to infinite frequency. So the procedure essentially involves determining the frequency response of the system and adding suitable circuits to the ouput to make the frequency response 'flat', ie amplitude independent of frequency. When this is done the inverse transfer function will have been determined.

Fig 33 shows the amplitude frequency characteristics of the transducer plus thruster. The peak at 26 Hz is the fundamental due to the thrust transducer. The small peaks and ripples of higher frequencies are caused by the thruster. The amplitude and frequency scales are linear. The pole at 26 Hz is removed by A^{-1} shown in Fig 19, this corresponds to the simple inverse transfer function discussed in section 3. Fig 34 shows the resultant frequency response and demonstrates why A^{-1} is inadequate on its own - there is a peak (or pole) at about 128 Hz followed by a zero at 141 Hz. The response of the system to an

impulse is shown in Fig 35 - the oscillations at 128 Hz are very apparent. Note
that in Fig 35 the oscillations at 260 Hz corresponding to the pole at 260 Hz in
Fig 34 have been removed to make the lower frequencies clear.

The pole at 128 Hz and zero at 141 Hz are smoothed by a transfer function
of the form

$$C(s) = \frac{P + \frac{Q}{q} sT + Rs^2T^2}{1 + \frac{1}{q} sT + s^2T^2} \tag{10}$$

and actual numerical values employed were:

$$C(s) = \frac{0.862 + 5.89 \times 10^{-8}s + 1.243 \times 10^{-6}s^2}{1 + 6.342 \times 10^{-8}s + 1.243 \times 10^{-6}s^2} . \tag{11}$$

The pole at 264 Hz is smoothed by a transfer function of the form

$$D(s) = \frac{1 + \frac{u}{q} sT + s^2T^2}{1 + \frac{1}{q} sT + s^2T^2} \tag{12}$$

and actual values employed were:

$$C(s) = \frac{1 + 8.3 \times 10^{-7}s + 3.544 \times 10^{-7}s^2}{1 + 1.5 \times 10^{-5}s + 3.544 \times 10^{-7}s^2} . \tag{13}$$

The values of uT/q and T/q in the numerator and denominator are somewhat
approximate since the q required was high (about 40) and the required value of
u was small (about 0.056) so it was found best to achieve these values by
slightly unbalancing the parallel T network used to achieve $D(s)$.

The two operations $C(s)$ and $D(s)$ are performed in series and the
practical realisation of $C(s)D(s)$ is shown in Fig 36. $C(s)D(s)$ consists of
two parallel T networks connected in series. In $C(s)$ the effect of a finite
q is obtained by c_1 and R_1 , and in $D(s)$ the effect of a finite q is
obtained by slightly unbalancing the network. The circuits of $C(s)$ and $D(s)$
(as well as $A(s)$ - Fig 19) have to be set up very carefully, all components
have a tolerance of 0.1% and then have to be trimmed to achieve the required
results. Fig 37 shows the effect of $C(s)D(s)$ on the system response. In
addition to $C(s)D(s)$ the response shown in Fig 9 has been tailored by a low
pass filter (described in 5.6) to define the bandwidth and also attenuate the

higher frequency resonances. The small residual ripples are difficult to remove
and do not greatly affect the system response.

The system $\left[\text{thrust transducer} \times A(s) \times C(s) \times D(s)\right]$ was used to obtain the
thrust data from a hydrazine thruster shown in Fig 29 and the frequency response
shown in Fig 37 is the corresponding system response. The amplitude frequency
curves Figs 33, 34 and 37 were obtained by exciting the thrust transducer by a
sinusoidally varying force of varying frequencies. This is readily achieved by
feeding a sinusoidal current through the calibrator coil (see section 6) and
recording the resultant amplitude from the displacement transducer.

REFERENCES

No.	Author	Title, etc.
1	D. Stott	The design and application of hybrid hydrazine resistojets. Conference on electric propulsion of space vehicles, Culham UK, April 1973, paper 9.3
2	C.K. Murch C.R. Hunter	Electrothermal hydrazine thruster development. AIAA paper 72-451 (1972)
3	A.H. Boyd	High response pulse rocket engine thrust measurement system. Instrumentation in the aerospace industry Vol 15 (1969) Proc. of the 15th international ISA instrumentation symposium
4	F.L. Crosswy H.T. Kalb	Investigation of dynamic rocket thrust measurement techniques. AEDC-TR-67-202 (1967)
5	F.L. Crosswy H.T. Kalb	Dynamic compensation and force calibration techniques for a static and dynamic thrust measurement system. AEDC-TR-68-202 (1968)
6	F.L. Crosswy H.T. Kalb	Performance of a dynamically compensated load cell force measurement system. AEDC-TR-68-211 (1968)
7	P.R. Geffe	Simplified modern filter design. London Iliffe Books Ltd., p.67 (1964)
8	D.J. Storey W.J. Cullyer	Active low-pass linear phase filters for pulse transmission. Proc. IEE Vol 112, No.4 (1965)
9	L.A. Zadeh C.A. Desoer	Linear system theory. McGraw-Hill, section 8.2, p.394 (1963)

Reports quoted are not necessarily available to members of the public or to commercial organisations.

Fig 1
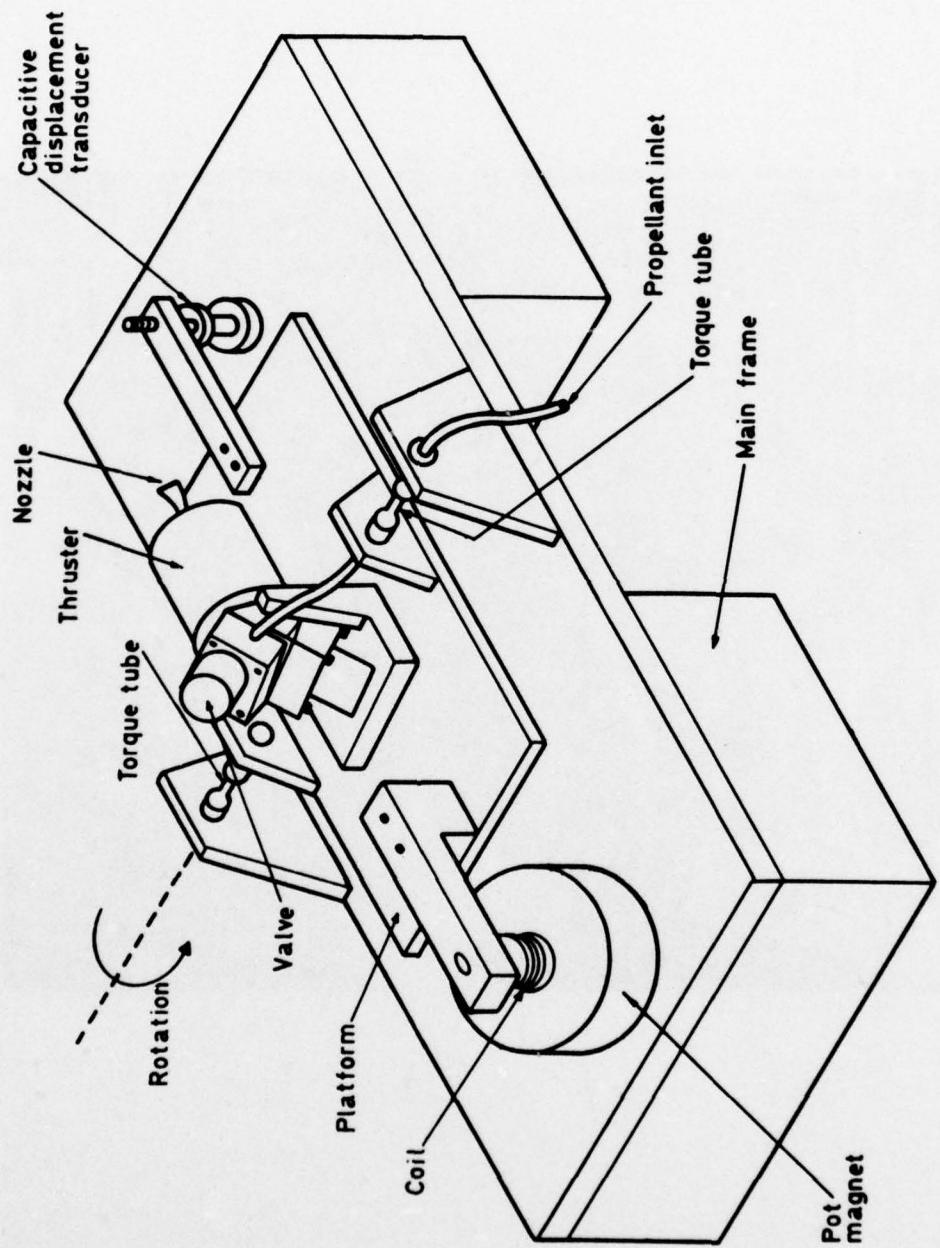
Fig 1   Thrust transducer schematic

TR 77025
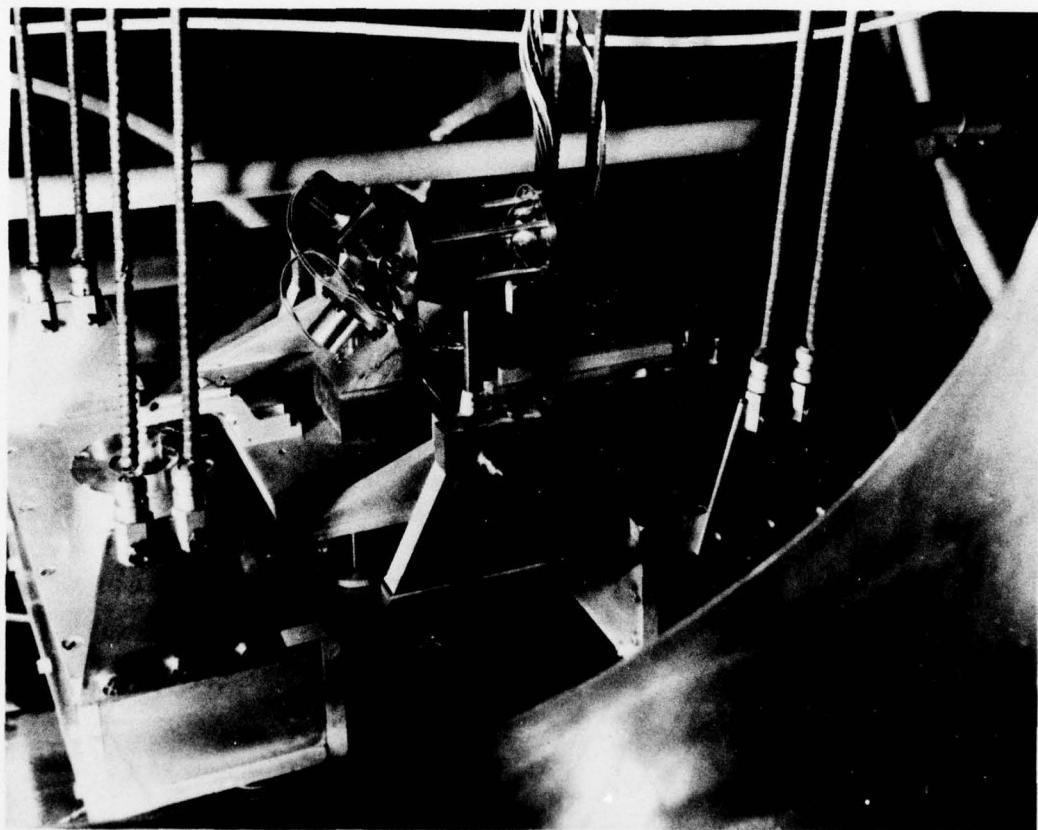
Fig 2

Fig 2   Thrust transducer installed in vacuum chamber

Fig 3

Pipe fitting

Nut

4 BA Dowty washer

0.25in x0.04in 'O' ring

Tube holder

Torque tube

x 4 Full scale
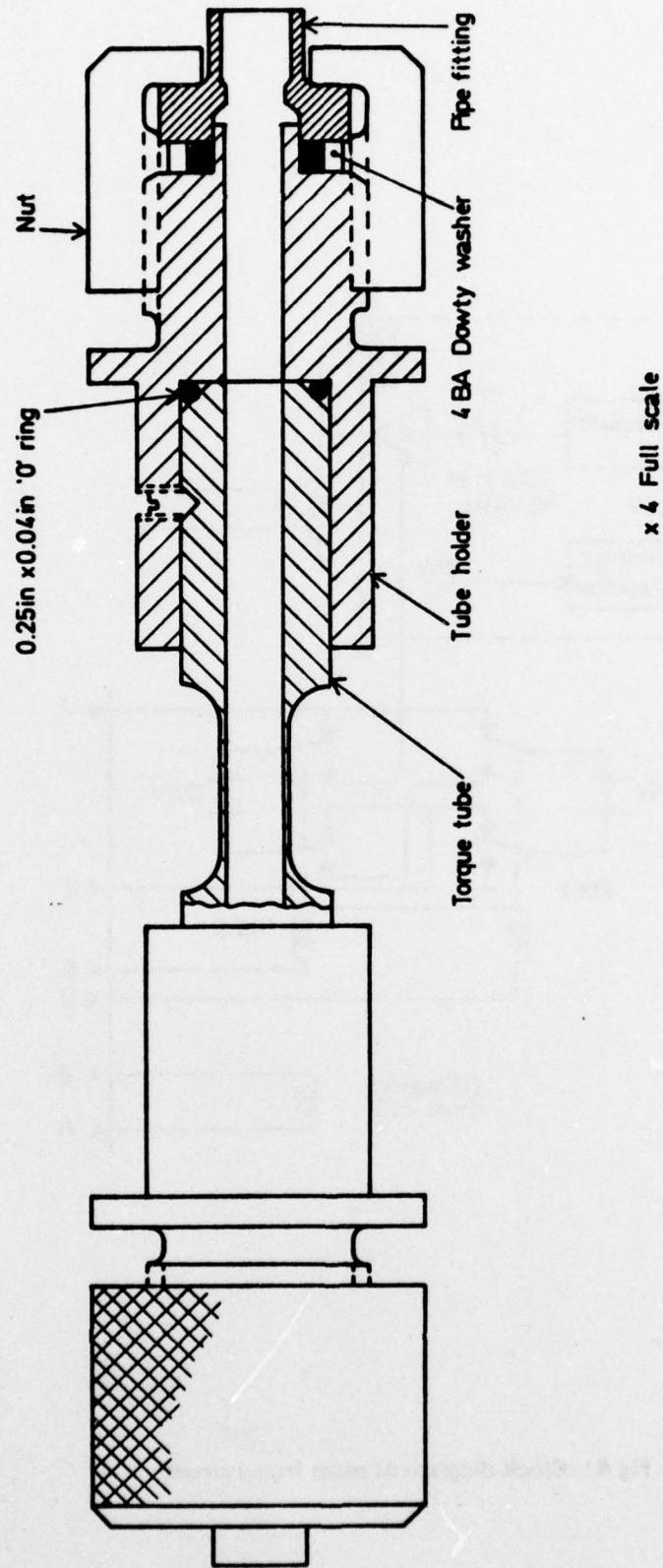
Fig 3   Torque tube assembly

Fig 4
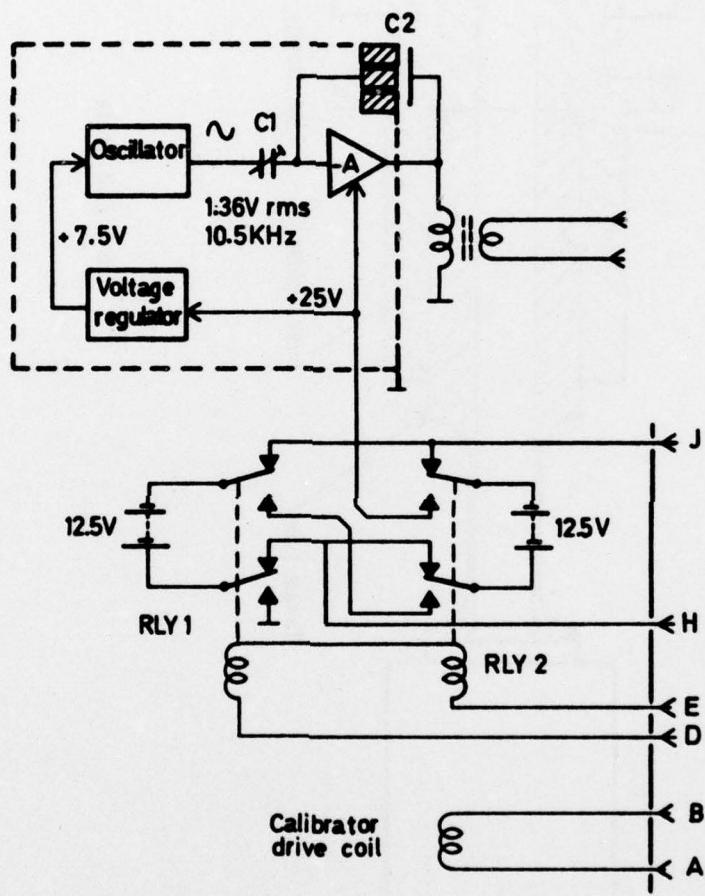
Fig 4   Block diagram of main frame circuit

Fig 5
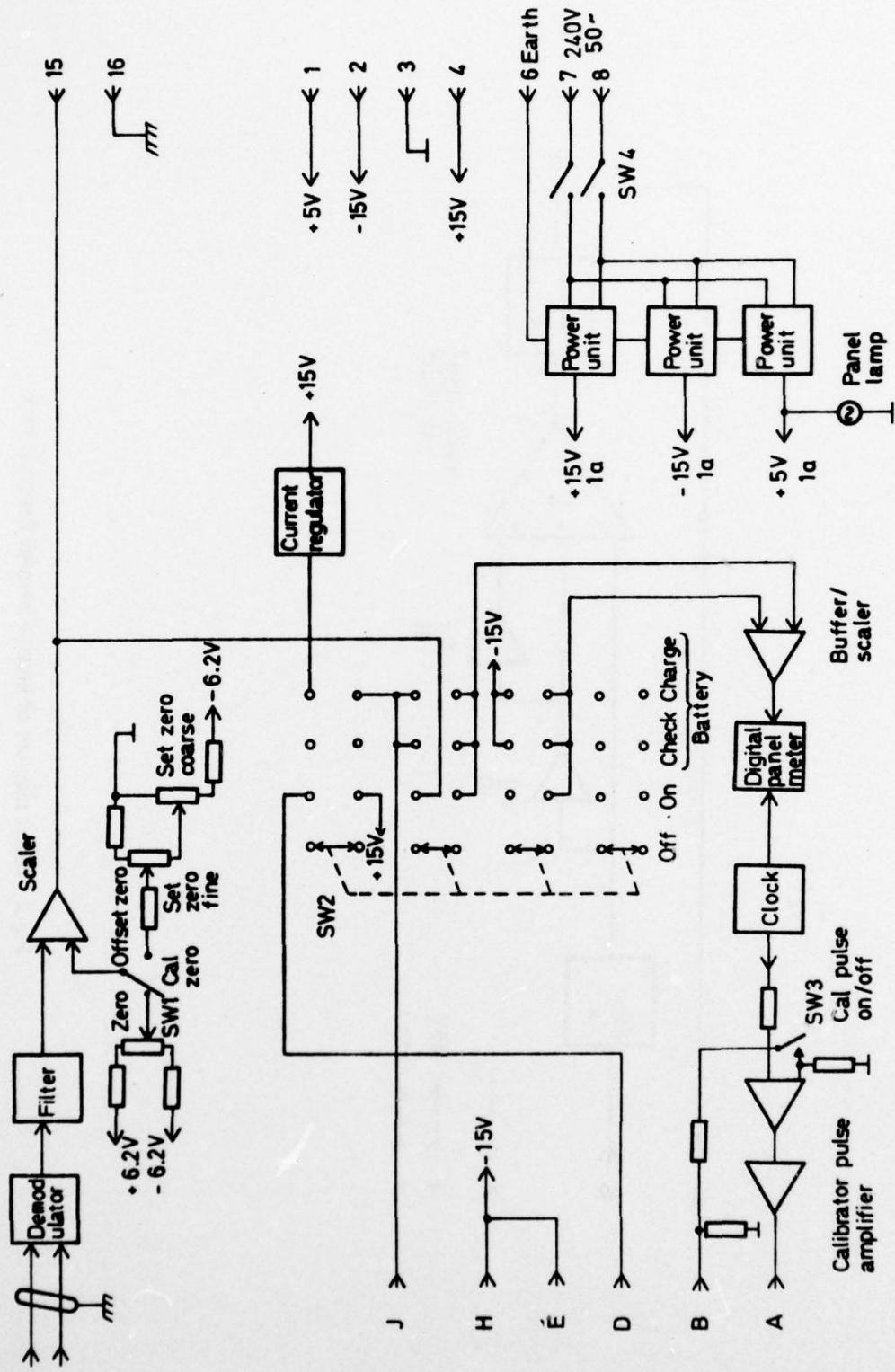
Fig 5   Block diagram of control unit

TR 77025
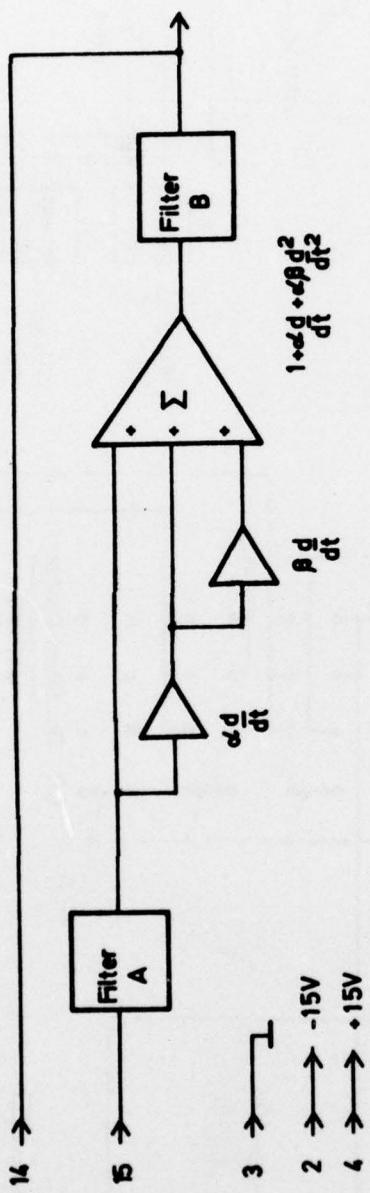
Fig 6

Fig 6   Block diagram of inverse transfer function unit
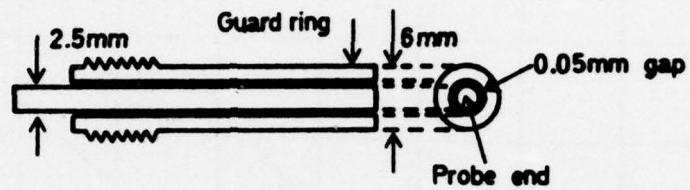
Fig 7   Probe schematic
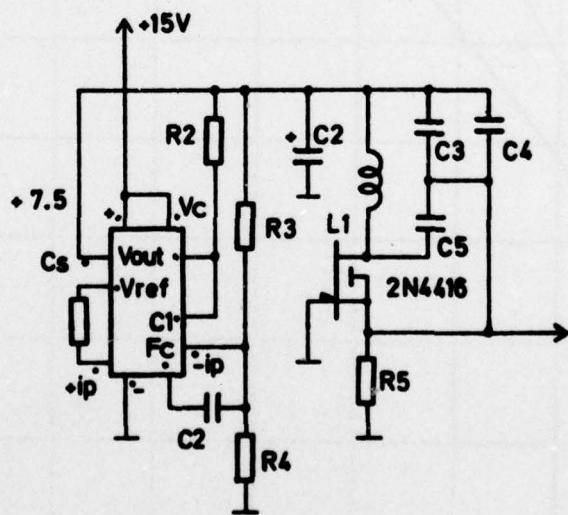
Fig 8   Oscillator

Fig 9
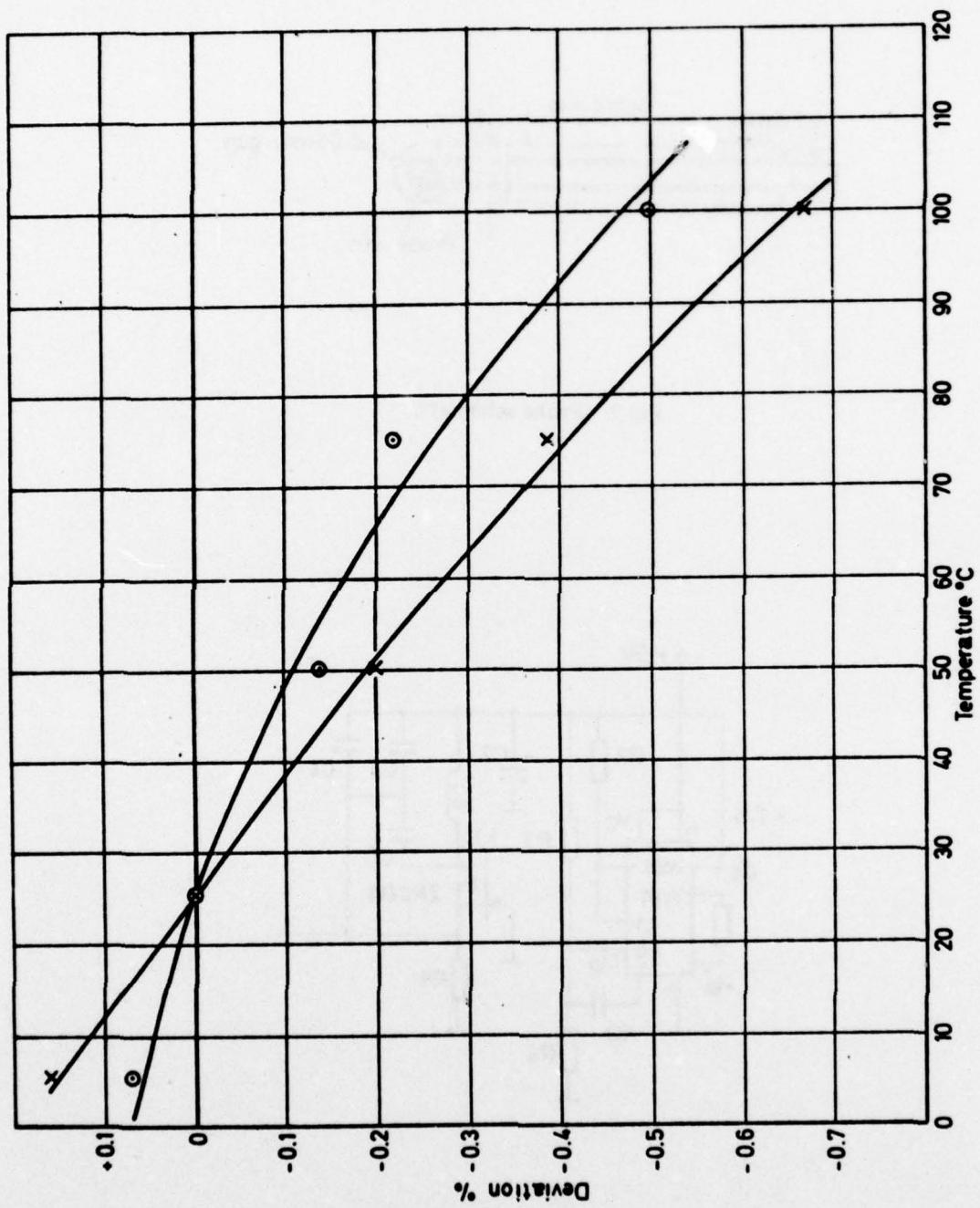
Fig 9   Oscillator output voltage amplitude deviation v temperature

Fig 10
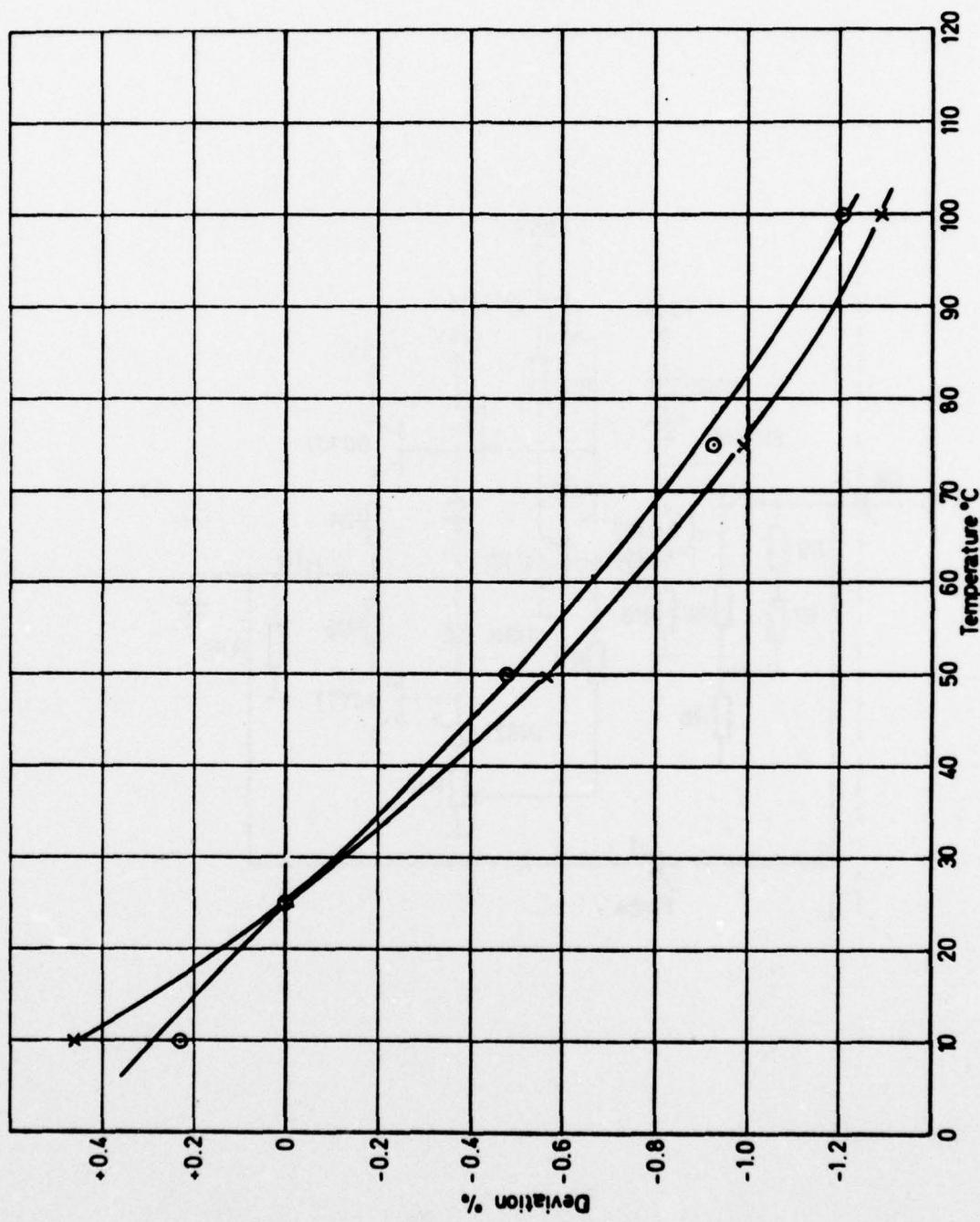
Fig 10 Oscillator output frequency deviation

Fig 11
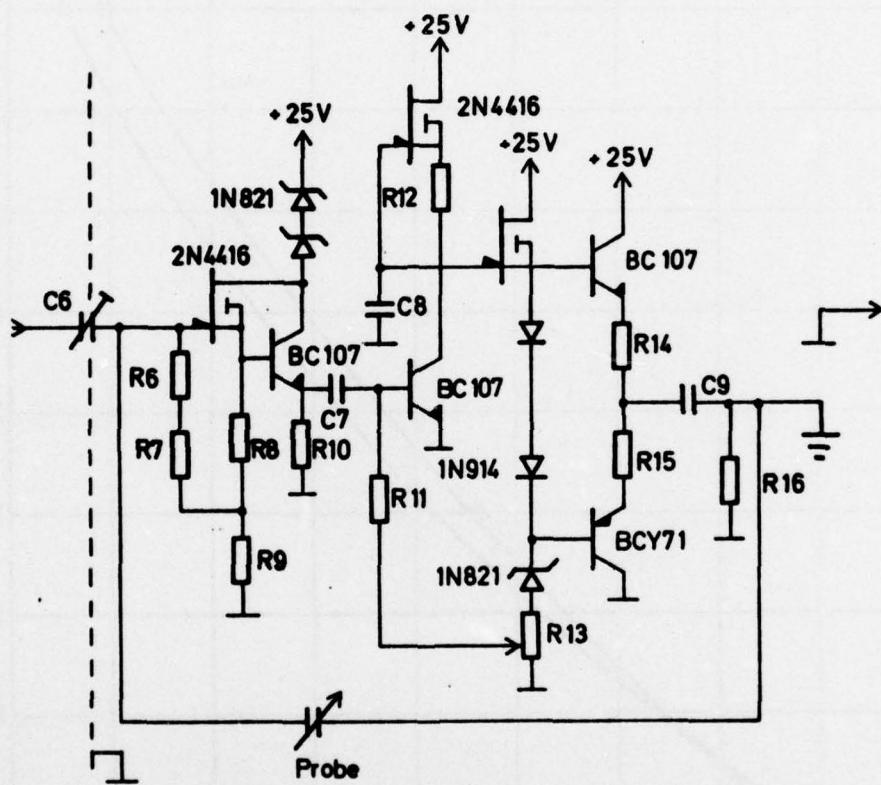
Fig 11   High gain amplifier

Fig 12
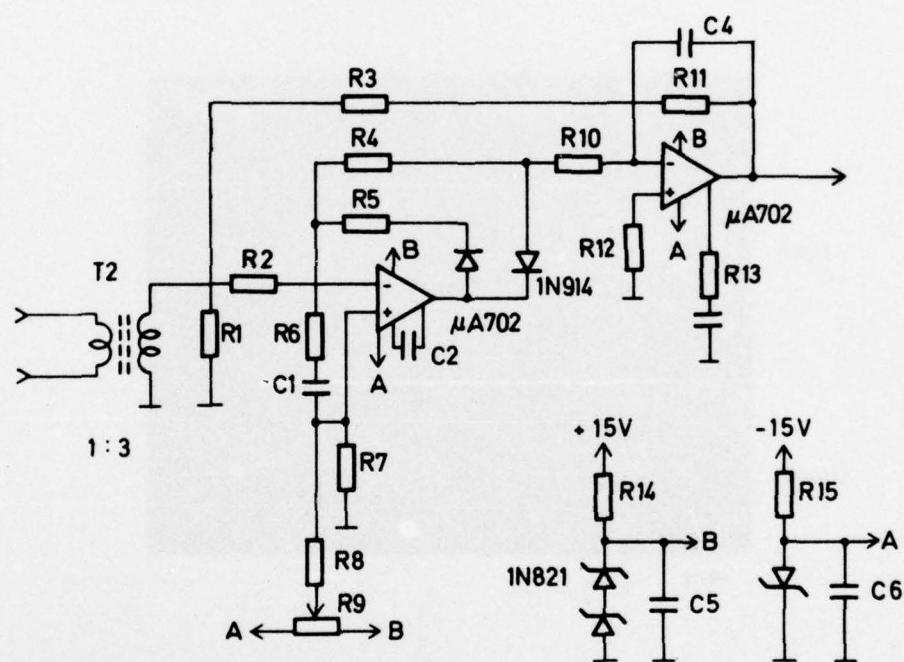
Fig 12   Rectifier

Fig 13

Input

Output

→ | | ← 200 μs
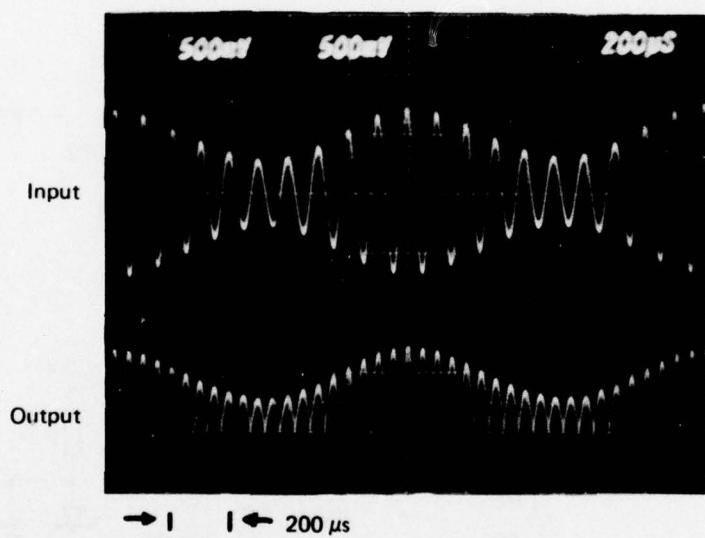
Fig 13   Rectifier input and output waveforms

Fig 14
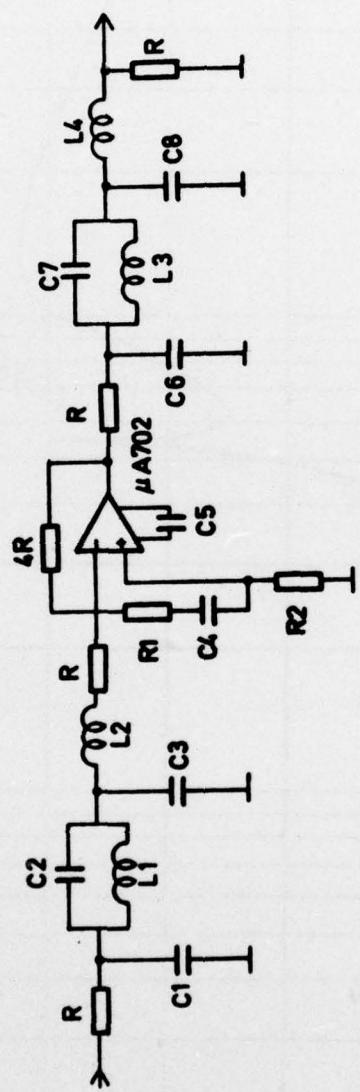
Fig 14   Demodulator filter circuit

Fig 15
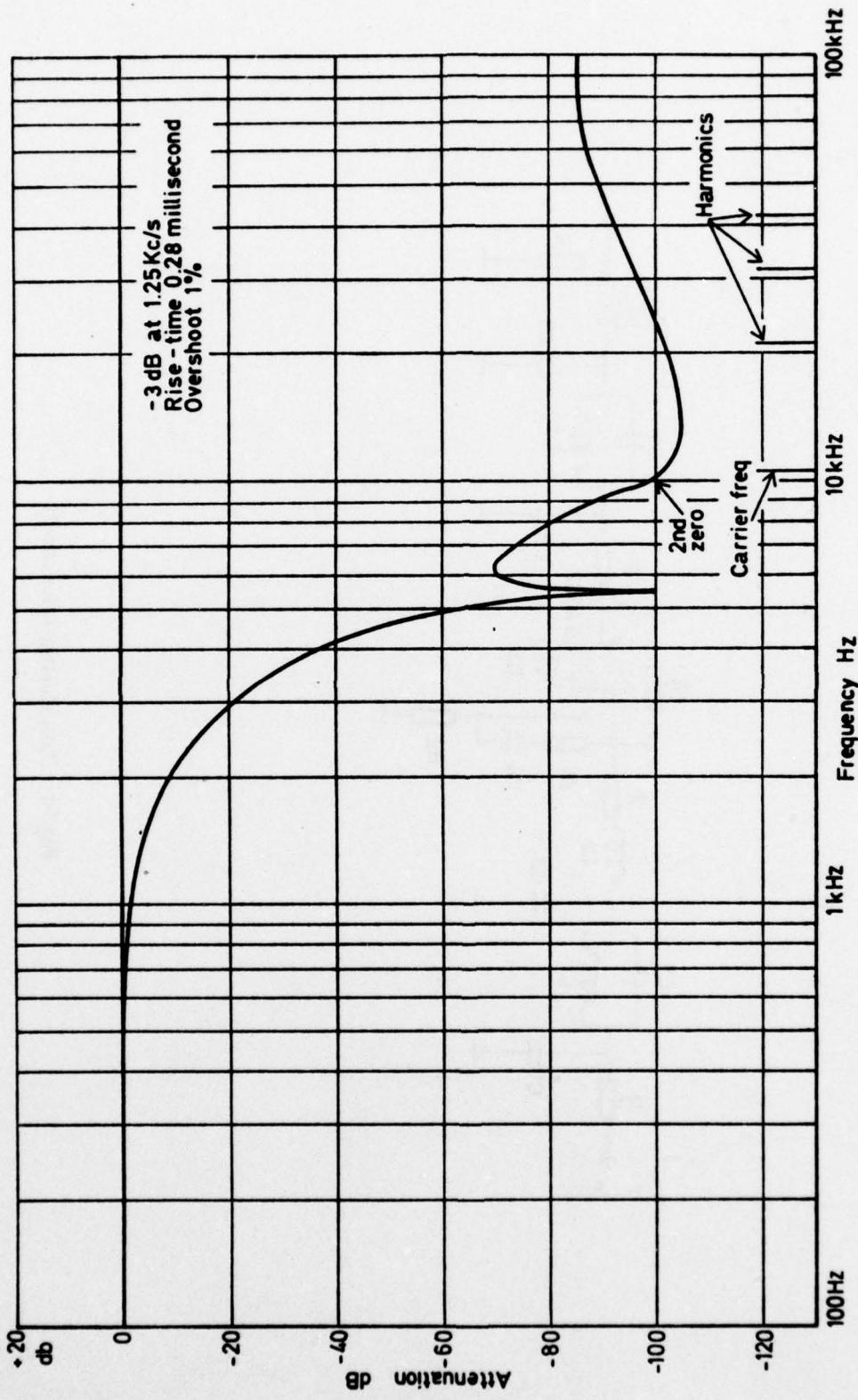
Fig 15 Demodulator filter frequency response
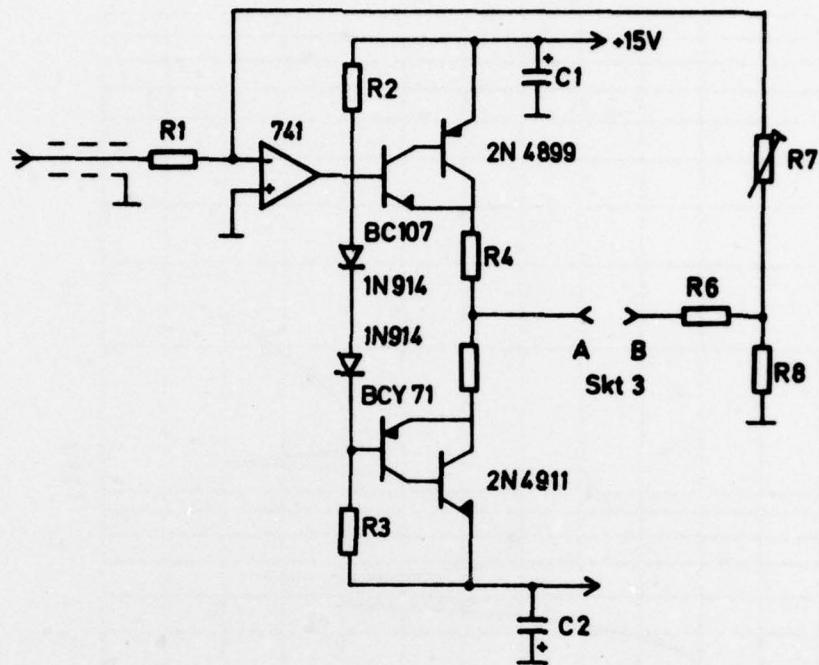
Fig 16   Calibrator circuit
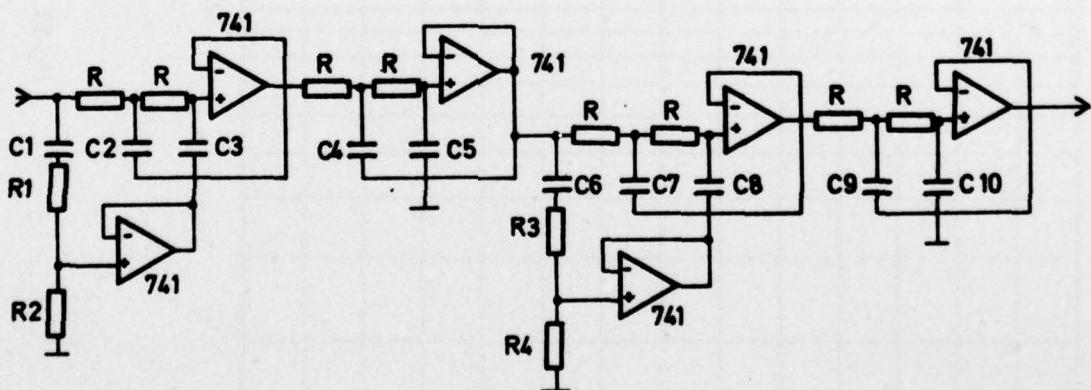
Fig 17   Filter A and Filter B circuits

Fig 18
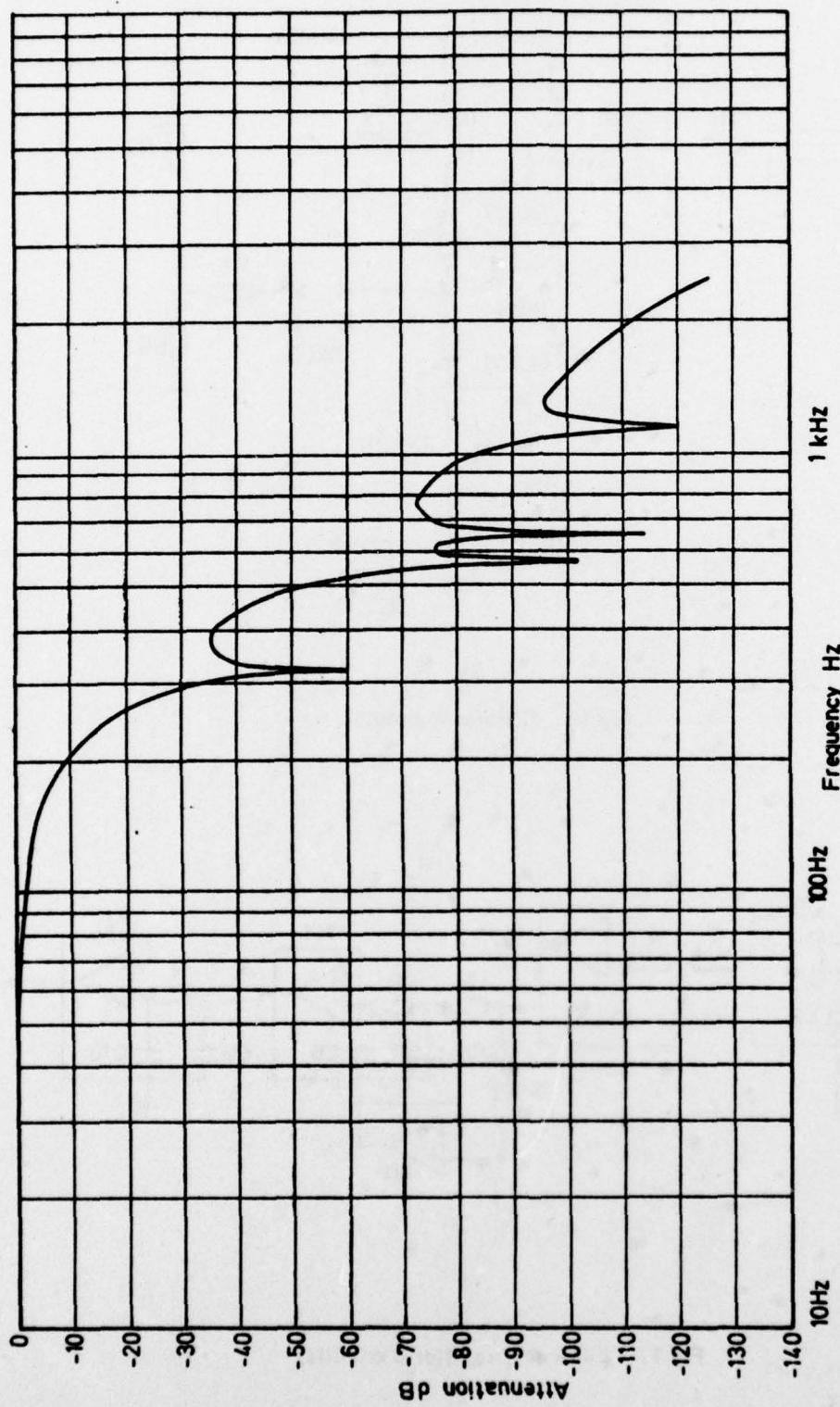
Fig 18   Filter A plus Filter B frequency response

$$V_{out} = \left[1 + C1\,R1\,\frac{R4}{R3}\cdot\frac{d}{dt} + C1\,R1\,C2\,R2\,\frac{R6}{R5}\cdot\frac{d^2}{dt^2} \right] V_{in}$$
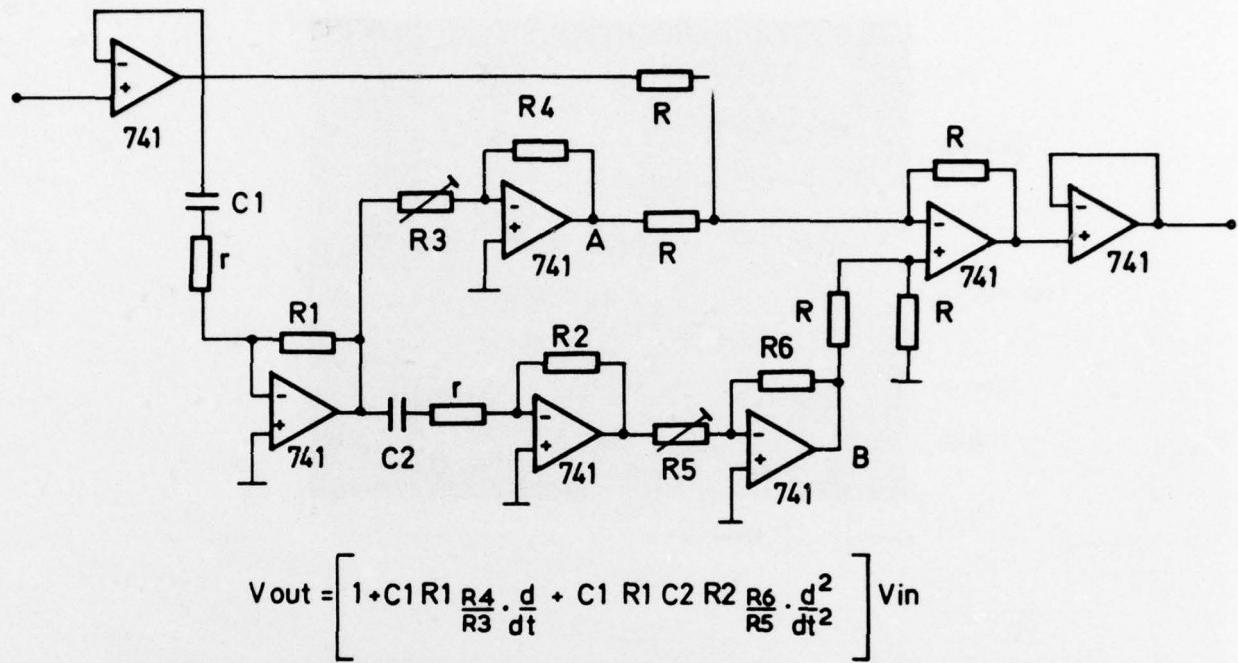
Fig 19   Inverse transfer function
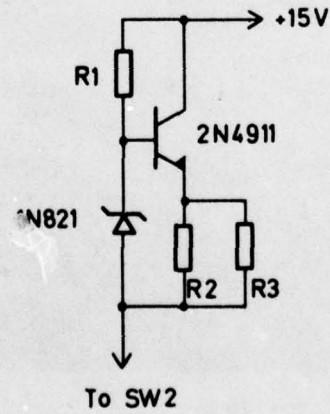
Fig 20   Battery current regulator

TR 77025
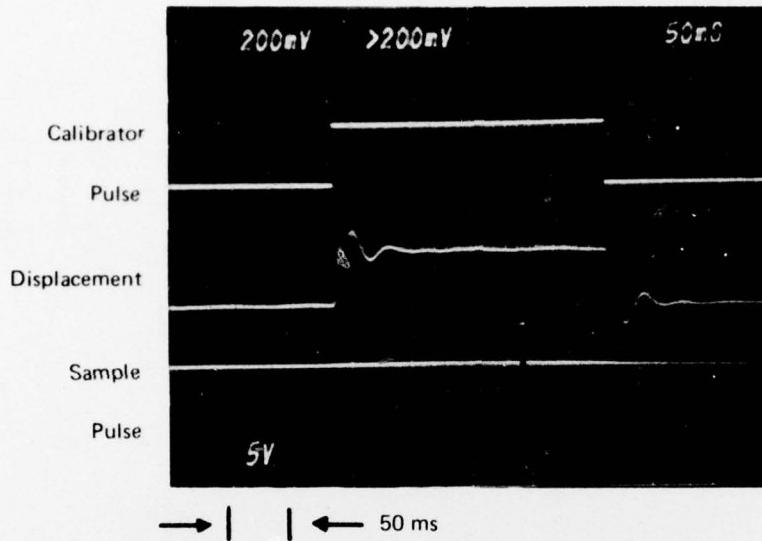
Fig 21   Calibrator, displacement and sampling waveforms
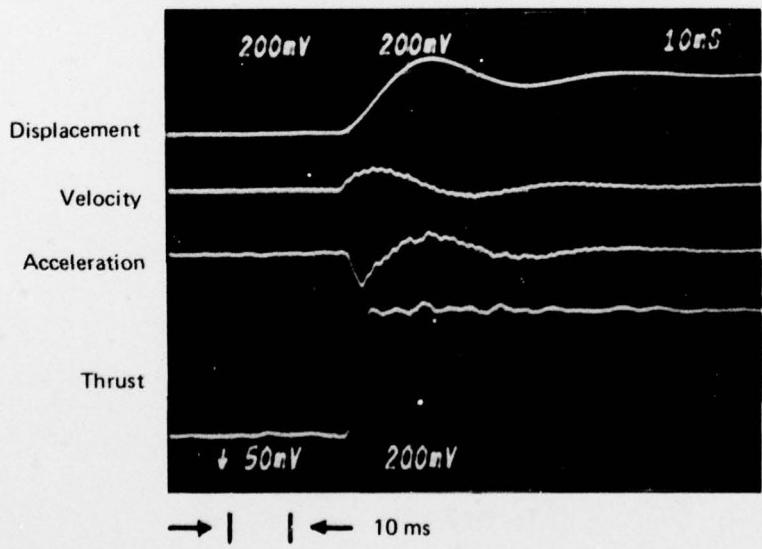
Fig 22   Inverse transfer function waveforms
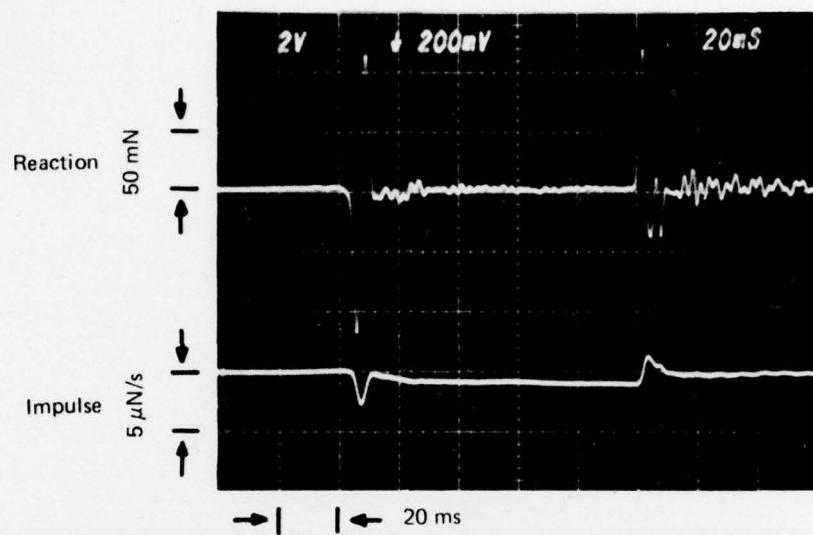
Fig 23   Valve reaction transients
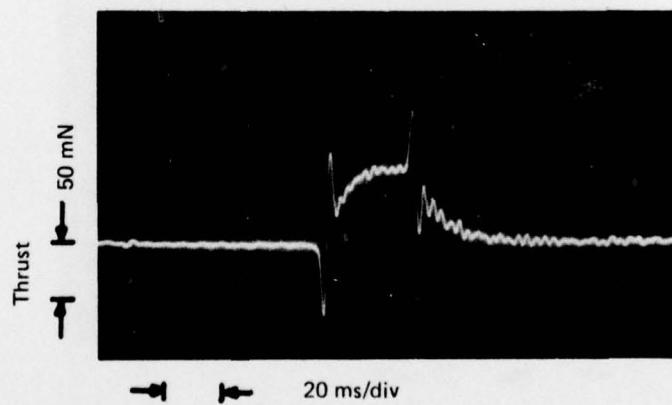
Fig 24   Resistojet thrust pulse: 2.5ms system rise time
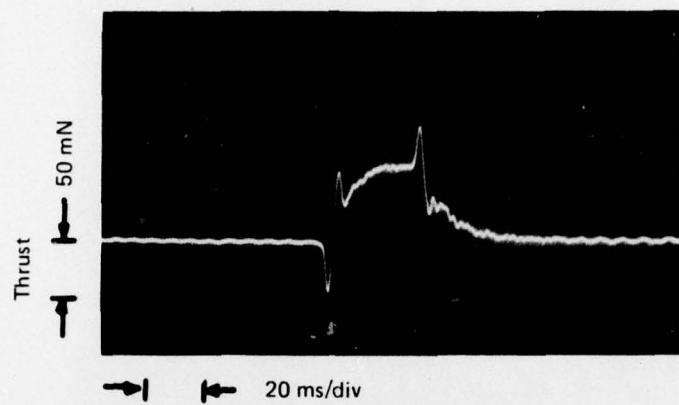
Fig 25   Resistojet thrust pulse: 5.0ms system rise time
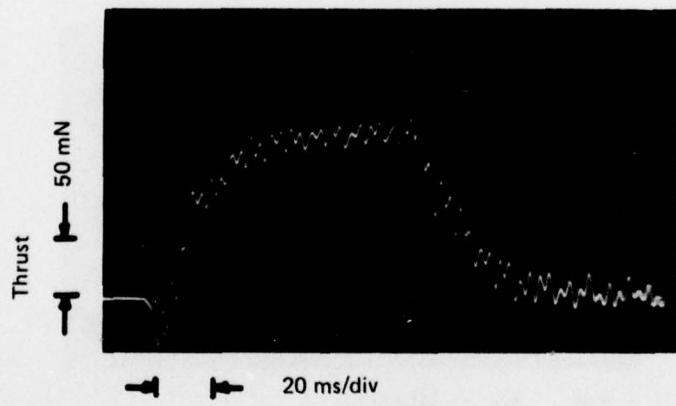
Fig 26   Resistojet thrust pulse with resonant mounting

TR 77025
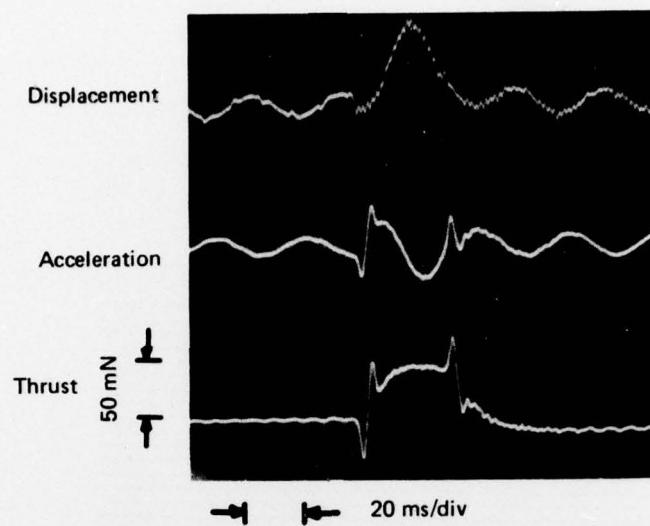
Fig 27   Inverse transform waveforms corresponding to thrust pulse in Fig 25
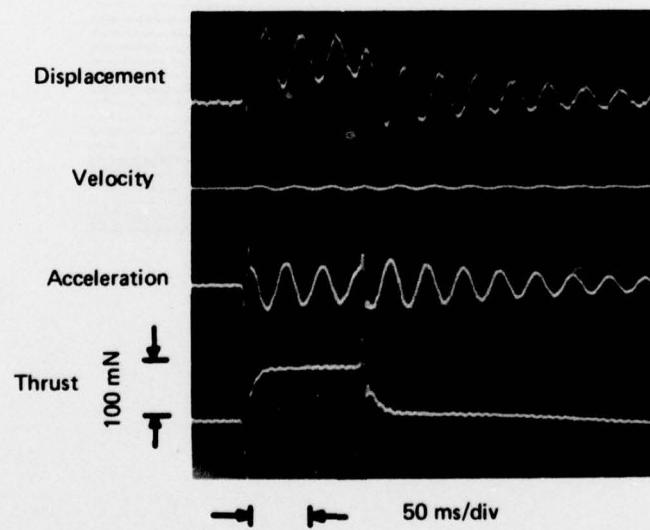
Fig 28   Inverse transform waveforms with damping

TR 77025
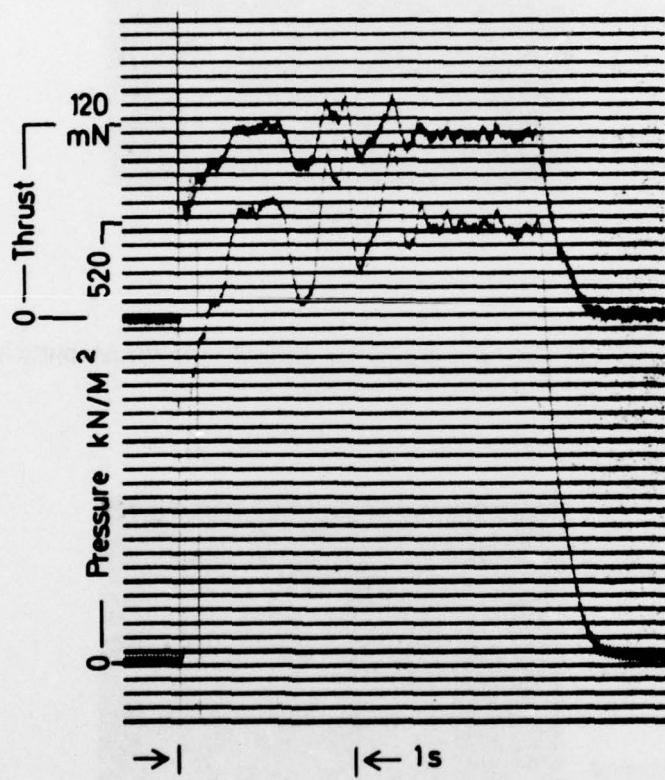
Fig 29

Fig 29 EHT thrust and pressure pulses

Fig 30

$$Vout = \frac{1}{RC}\int_{0}^{t} \Delta Vin \ dt$$
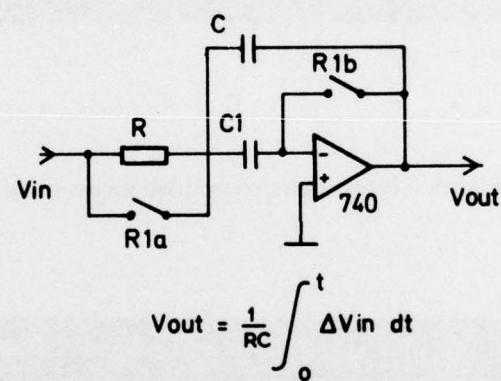
Fig 30   Impulse integrator
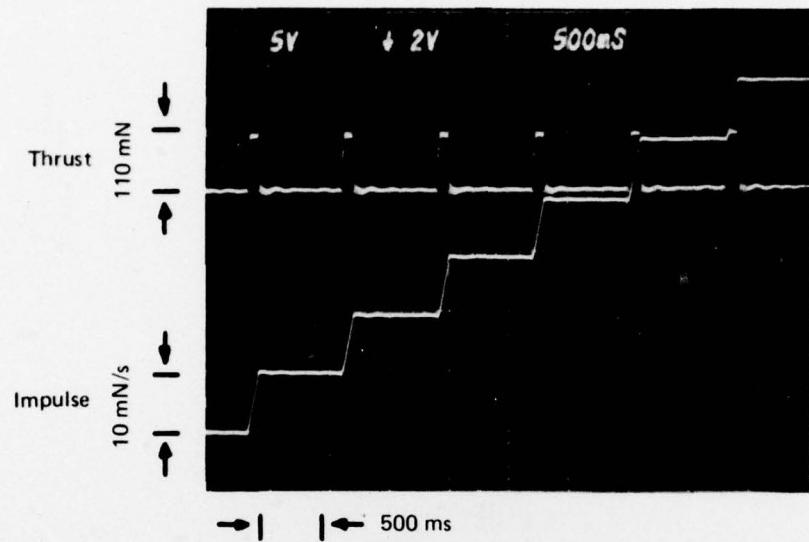
Fig 31   Integrated consecutive thrust pulses
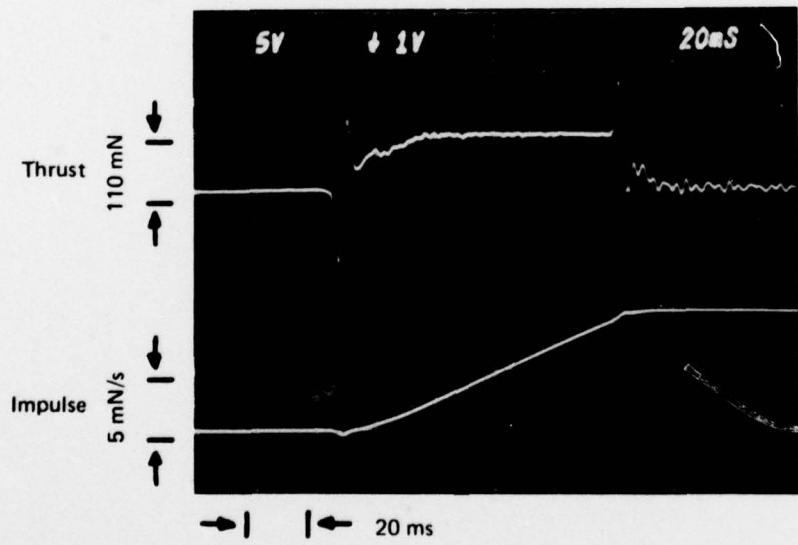
Fig 32   Impulse produced by single thrust pulse

Fig 33
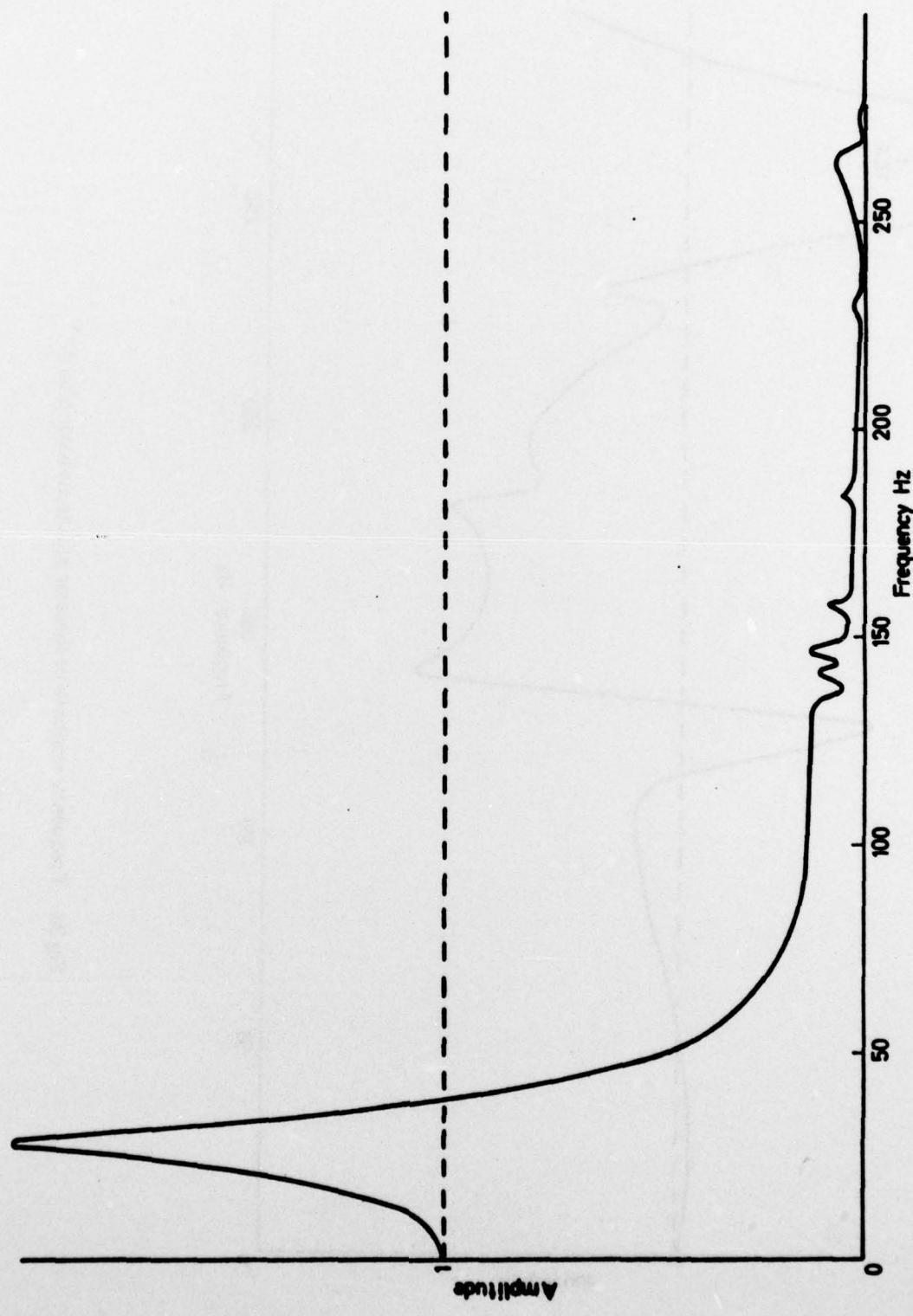
Fig 33   Frequency characteristic of thruster plus transducer
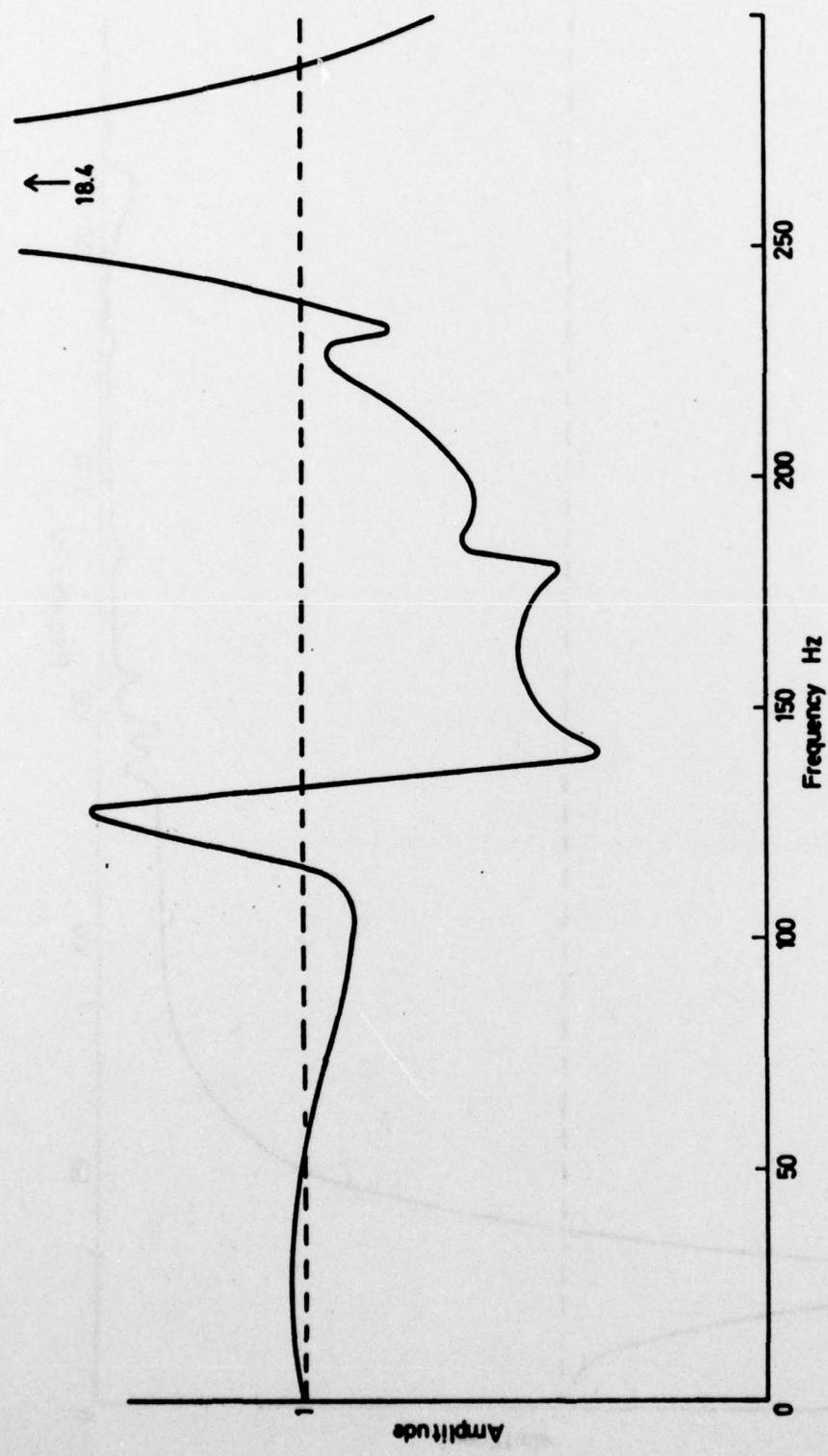
Fig 34   Frequency response of thruster plus transducer plus A^{-1}
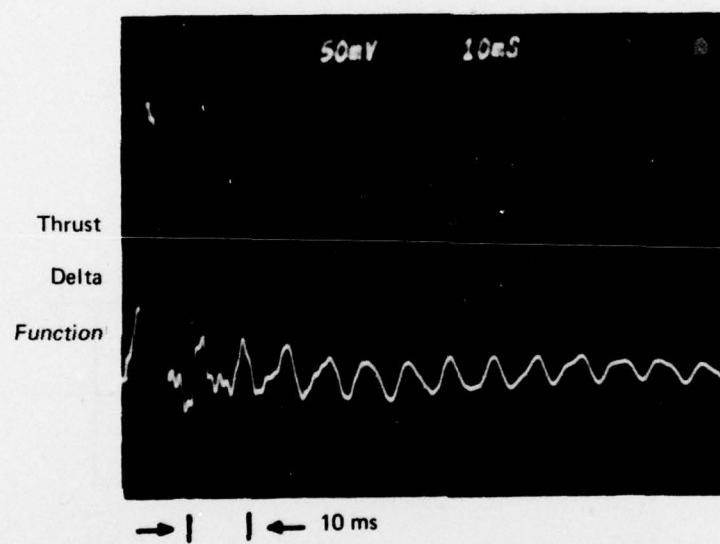
Fig 35

Fig 35   Impulse response corresponding to frequency response shown in Fig 34

Fig 36


R1 C1
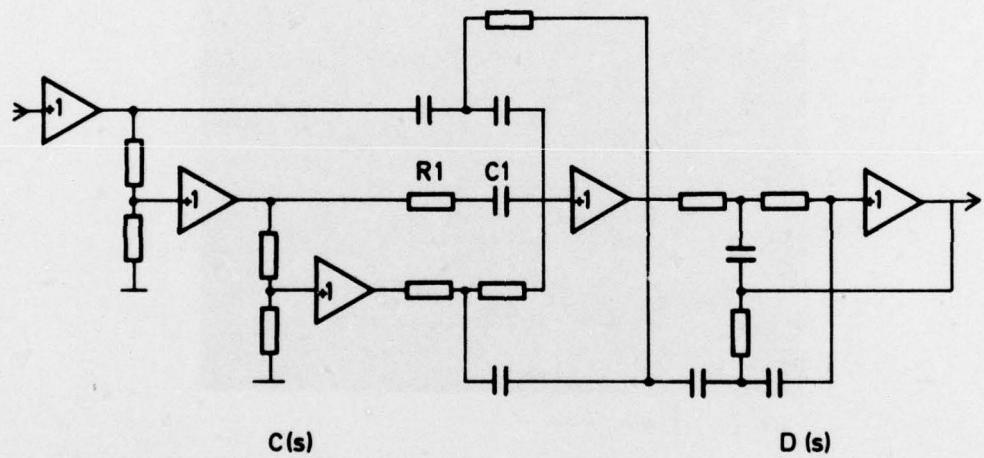
C(s)   D (s)

Fig 36   System C(s) x D(s)
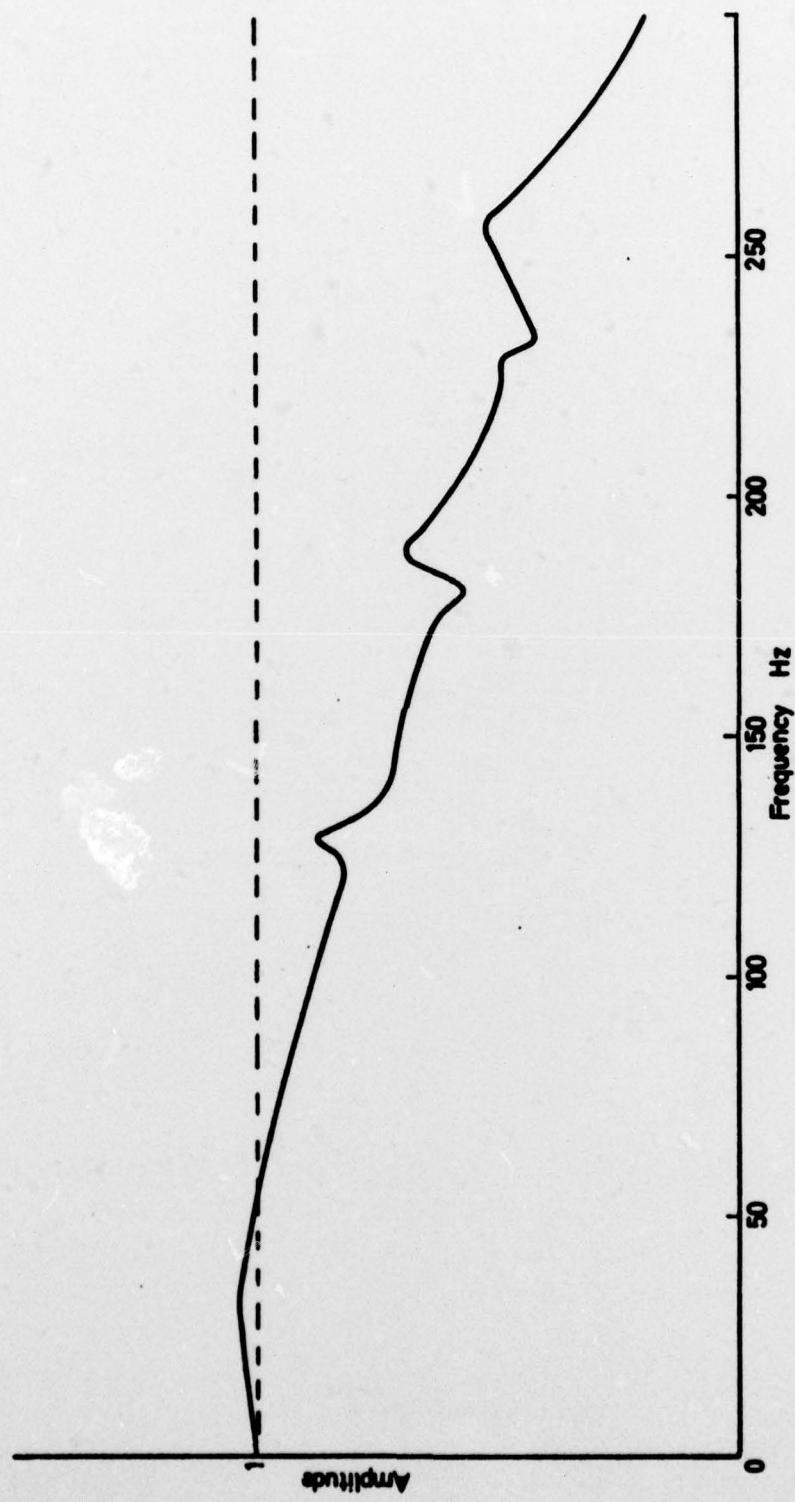
TR 77025

Fig 37

Fig 37   Response of system [thrust transducer x A(s) x C(s) x D(s)]